Formability characterization of AISI202 Stainless Steel

Submitted by
Prahlad Kumar Tewari
2K13/PIE/26
Part-Time

***In partial fulfilment for the award of the degree* of**

MASTER OF TECHNOLOGY in PRODUCTION ENGINEERING

Submitted to
Delhi Technological University (DTU)
Formerly Delhi College of Engineering
Shahbad Daulatpur Road
Bawana, Delhi-110042

Table of Contents

List of tables

List of Figures

Acknowledgement

I wish to express my sincere gratitude to **Dr. R. K Pachauri**, Ex Director General, The Energy and Recourses Institute (TERI), for allowing me to carry out MTech (Part-time) in Production Engineering at Delhi Technological University (DTU). I am also grateful to **Dr. Ajay Mathur**, Director General, The Energy and Recourses Institute (TERI), for his kind consent to continue my MTech course at DTU.

I would like to express my deep and sincere gratitude to my senior **colleagues Dr. Malini Balakrishnan**, Senior Fellow, and **Dr. Vidya S Batra**, Senior Fellow & Area Convenor, for their kind understanding, guidance, support and encouragement. I feel extremely fortunate to have got chance to work with them. I would also like to thank my colleagues (**Dr. Subhankar Basu, Mr. Ravikaran Singh, Mr. Rajeev Pillai, Ganesh Chandramouli, and Keerthika Mandava**) at The Energy & Resources Institute (TERI) to their constant support. I am particularly thankful to **Keerthika Mandava** for all her kind help and encouragement.

I would like to express my immense gratitude to my guides, **Mr. Vijay Gautam,** Assistant Professor and **Dr. A.K Madan**, Professor, Department of Mechanical & Production Engineering, for their constant guidance and encouragement which helped me to complete my research project in the best way possible. I am highly grateful to **Mr. Vijay Gautam** for his kind advice and his availability for discussions throughout my research work which enabled me to overcome many difficulties. I would also to thank **Mr. Omprakash and Mr. Tekchand**, DTU for helping me perform my experiments at DTU, New Delhi.

My humble thanks to **Prof. D. Ravi, Prof. P.V.M Rao, Dr. Hariharan**, Indian Institute of Technology (IIT), Delhi for their kind consent to use facilities at IITD to carryout my experiments and simulations in their respective labs at IIT Delhi. I am particularly thankful to **Dr. D Ravi** for his valuable advice on formability characterization of my specimens. I would also to thank **Mr. Vedprakash, Mr. D. Satish Raja and Mr. Amit**, Research Scholars at IIT, Delhi for their kind help in carrying out stretch forming experiment and simulation at IIT Delhi. I am really thankful to **Mr. Vedprakash** for his constant help. I would also to thank **Mr. Ramchandran**, NC Lab incharge at IIT, Delhi for providing me facility to perform my experiments.

I would like to express my deep gratitude to **Mr. Madanji Bansali**, Monika Udyog, Ahmedabad, for kindly providing SS sheets for carrying out formability characterization test. I would also acknowledge my **car DL2CAN4937** for being my sarthi of about 85 km in each class day at DTU. I wish to thank everyone whom I could not mention in my acknowledgement but have provided their support, understanding and encouragement.

I do not have any words to express my gratitude to my **family members** for all their unconditional support, endless love, patience and blessings during my study. Thank you **Papa, Mummy, Neelam, Govindji and Shruti.** My humble thanks to my **Dadi** for her constant blessings.

Last but not the least, I humbly thank the **Almighty** for being so kind to me and pray that everyone is bestowed with opportunities and capabilities to fulfil their dreams.

Prahlad Tewari

2K13/PIE/26

MTech Part-Time

Certificate by the Student

This is to certify that the MTech Thesis titled "**Formability characterization of AISI202 stainless steel**" is original work being carried out by me and has not been submitted anywhere else for the award of any degree.

Date:

Student

Prahlad Kumar Tewari

2K13/PIE/26

Date:

Submitted to

Dr. Vijay Gautam and Dr. A. K Madan

Department of Mechanical Engineering

Delhi Technological University (DTU)

Shahbad Daulatpur, Bawana Road,

Delhi – 110042

1. Title of the Project

Formability characterization of AISI202 stainless steel

2. Publication

3. Objectives of the study

- To perform tensile tests to determine mechanical properties such as Yield Strength (YS), Ultimate Tensile Strength (UTS), Percentage Elongation
- To perform anisotropy test to determine planar and normal anisotropy
- To study the effect of plastic strain rate on anisotropic behaviour of AISI202 stainless steel
- To observe the microstructure of AISI202
- To experimentally determine the forming limit diagram(FLD) of AISI202
- To use finite element analysis (FEA) to predict failure of AISI202

4. Introduction

4.1 Stainless steel manufacturing

As per the World Steel Association, India was the third largest producer of steel in the world, producing about 89.58 million tonnes of crude steel during the year 2014 - 2015 (WSA, 2015). Out of which about 70% of long steel products are produced from steel rerolling industries, which are mostly small and medium sized enterprises (SMEs). Indian steel re-rolling sector comprises of over 1800 SMEs spread across the country. These SMEs are being operated in various clusters located across the country. In one such cluster in Ahmedabad, about 90 small scale stainless steel re-rolling mills are operational in various locations involving Vatva, Odhav, Naroda, Chatral and Kalol industrial areas. This cluster consist of 90 steel re-rolling mills, out of which about 25 mills are doing hot rolling of stainless steel flats and about 65 mills are engaged in cold re-rolling and annealing operations. In simple terms, hot rolling mills symbolize hot rolling of plates while cold rerolling mills symbolizes cold rolling of sheets. In technical terms, hot rolling is the heating the plates at a temperature above 1000-1200 ^{o}C in a reheating furnace and rolling the plates in red hot condition to a thickness of approximately 16 gauge. The rerolling process involves reheating the same 16 gauge sheet in a separate reheating furnace to an annealing temperature of around 900 ^{o}C. These annealed sheets are then pickled (acid cleaned) through various stages to obtain an intermediate product, free of scales and contamination. These pickled, scale-free sheets are then rolled in cold condition to achieve gauge reduction from 16 to 24 gauge, depending upon the customer requirement. Typical manufacturing process undertaken by the cold rolling mills is depicted in the process flow chart (Figure 1).

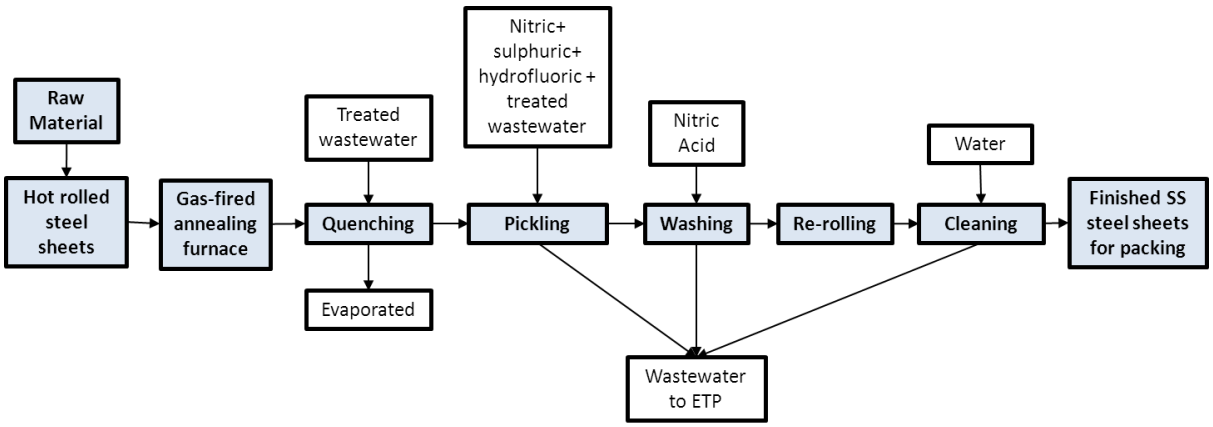

Figure 1: Typical manufacturing steps followed for cold rolling of SS sheets

With an estimated monthly production of about 30000 MT of SS sheet, the cluster is estimated to provide direct employment to about 6500-7000 individuals in the cold rolling mills and about 1000 individuals in hot rolling mills. Apart from this, the industry provides an indirect employment to about 350000 individuals associated with various manufacturing processes and allied works. The customers for these cold rolled SS sheets are utensil, pipes, hardware and kitchenware manufacturers located at various locations within the country and abroad.

For the purpose of MTech thesis work, the stainless steel AISI 202 was obtained from Monika Udyog, 6/1, GIDC, Phase-1, Vatva, Ahmedabad. The company is engaged in the manufacturing of 7-8 tonne per day (TPD) annealed and cold rolled SS sheets of 22 (about 0.8mm) gauge or 22 (about 0.6 mm) gauge depending upon customer requirement. Above SS sheets are obtained after sequential gauge reduction from 16 gauge (about 1.4 mm) sheets which the company receives from hot rolling mills as a raw material. The unit has multiple 4 high rolling mills and a roller hearth type annealing furnace with a capacity of 35 TPD. Furnace operates for 24 hours per day. Various rerolling facilities and broad working sequence is depicted in Figure 2.

Raw material (16 gauge (1.4 mm)) sheets received from hot rolling mills

Annealing furnace used for annealing of sheets at various stage of thickness reduction

Figure 2: Various cold rerolling facilities at Monika Udyog

4.2 Sheet metal forming, its applications and challenges

Formability is the ability of sheet metal to undergo shape change prior to failure by necking or tearing (excessive thinning). Sheet metal forming is a process in which flat thin blanks are deformed permanently to produce a wide range of products ranging from simple bending to stretching, to deep drawing of complex three dimensional parts. These operations are widely used in industry and hence knowledge of various sheet metal forming processes is essential to manufacture good quality products. However, it is very important to determine the extent to which a material can be deformed safely for designing a reproducible forming operation (Gedney R, 2002).

Numerous parts / objects are made by sheet metal operations, the most commonly used sheet metal parts includes automobile body panels, fuel tanks, aircraft parts, electrical panels, utensils, home and office storage cabinets, cabinets of various appliances such as CPU, UPS, home appliances, beverage cans, etc.

The major challenge faced by the sheet metal forming industry is increasing demand on lower consumption and lower CO_2 emissions. This has led to highest challenge on the weight reduction and light weight construction with the increased safety requirement. High strength steels are being widely used to meet above challenges, however, the application of high strength steel often leads to formability problems (Koacs et al., 2012).

Various sheet metal forming operations are being employed by the industry to produce useful objects.

4.3 Major sheet metal forming processes

4.3.1 Stretching

Stretch forming is the process in which the sheet material is stretched over a tool or a form block. The flange of the blank is securely clamped by jaws and a rigid punch or a form block pushes the sheet to get the desired punch shape. Higher blank holding forces are applied to prevent the flange portion from drawing into the die cavity. This process is extensively used in aircraft industry to produce parts having large radius of curvature and automotive body panels.

Salient features:

- Sheet metal is clamped at edges and stretched over a die or form block
- Dies made of zinc alloys, steels, plastics, wood
- Little or no lubrication
- Low-volume, versatile, and economic production
- Products: aircraft wing skin panels, automobile door panels, window frames

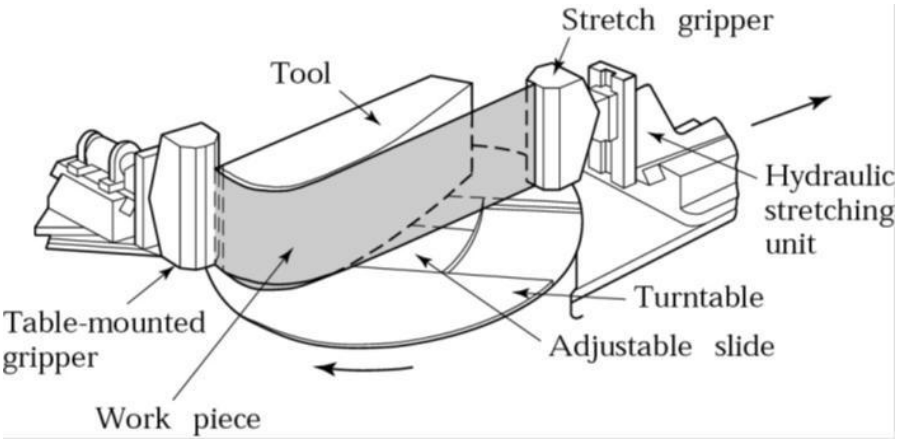

Figure 3: Schematic of typical stretch forming operations (Source: Cyril Bath Co.)

4.3.2 Deep drawing

Deep drawing is used for producing cup shaped parts with significant depth. This process is widely used in automobile industry. Here the material of appropriate size is drawn into a die by means of a punch. Blank holder force is used to press the blank against the die to prevent wrinkling and control the material flow into the die cavity. In deep drawing, the thickness of the cup wall is not constant. It is minimum near the cup bottom and maximum at the top of the cup.

Salient features:

- Wrinkling is caused by compressive (hoop) stresses that are induced as the blank moves into the die cavity
- Blank-holder (or hold-down ring) pressure must be correct
- Too much pressure causes tearing, too little causes wrinkling
- Typically 0.7-1.0% of the sum of the UTS and yield strength
- If Do-Dp< 5T, deep drawing may be successfully achieved without a blank-holder

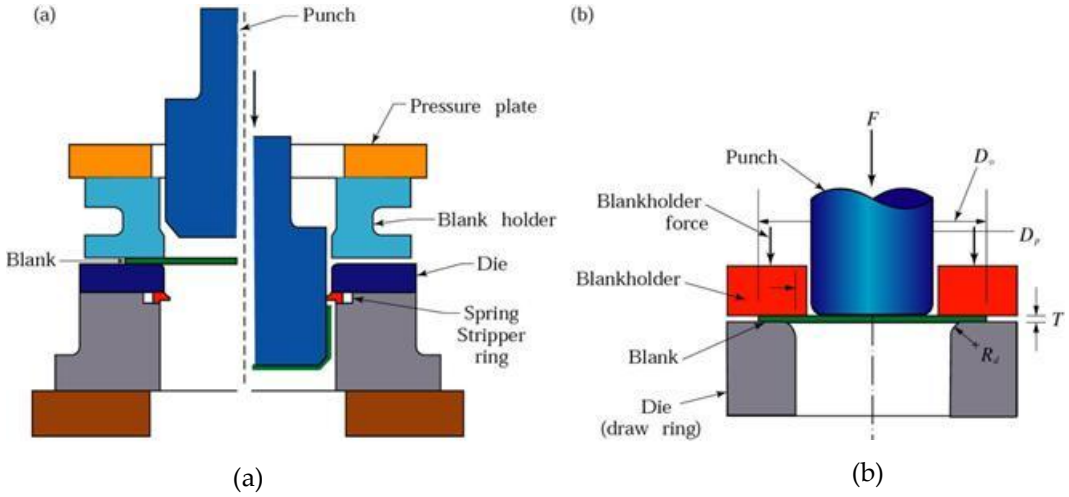

Figure 4: (a) Schematic illustration of deep-drawing process on a circular sheet metal bank (b) Process variables in deep drawing (Source: Kalpakjian.S, Schmid.S.R., Manufacturing Engineering and Technology, 2006, 4th Edi, Pearson Edu.)

4.3.3 Ironing

Ironing is used to reduce wall thickness in a deep drawn part. The cup height is increased at the expense of wall thickness, making the wall thickness more uniform. This can be achieved by forcing the cylindrical cup through an ironing die in which the punch-die clearance is smaller than the metal thickness. Usually drawing and ironing dies are combined in series so that uniform thickness of drawn cup can be obtained in a single pass.

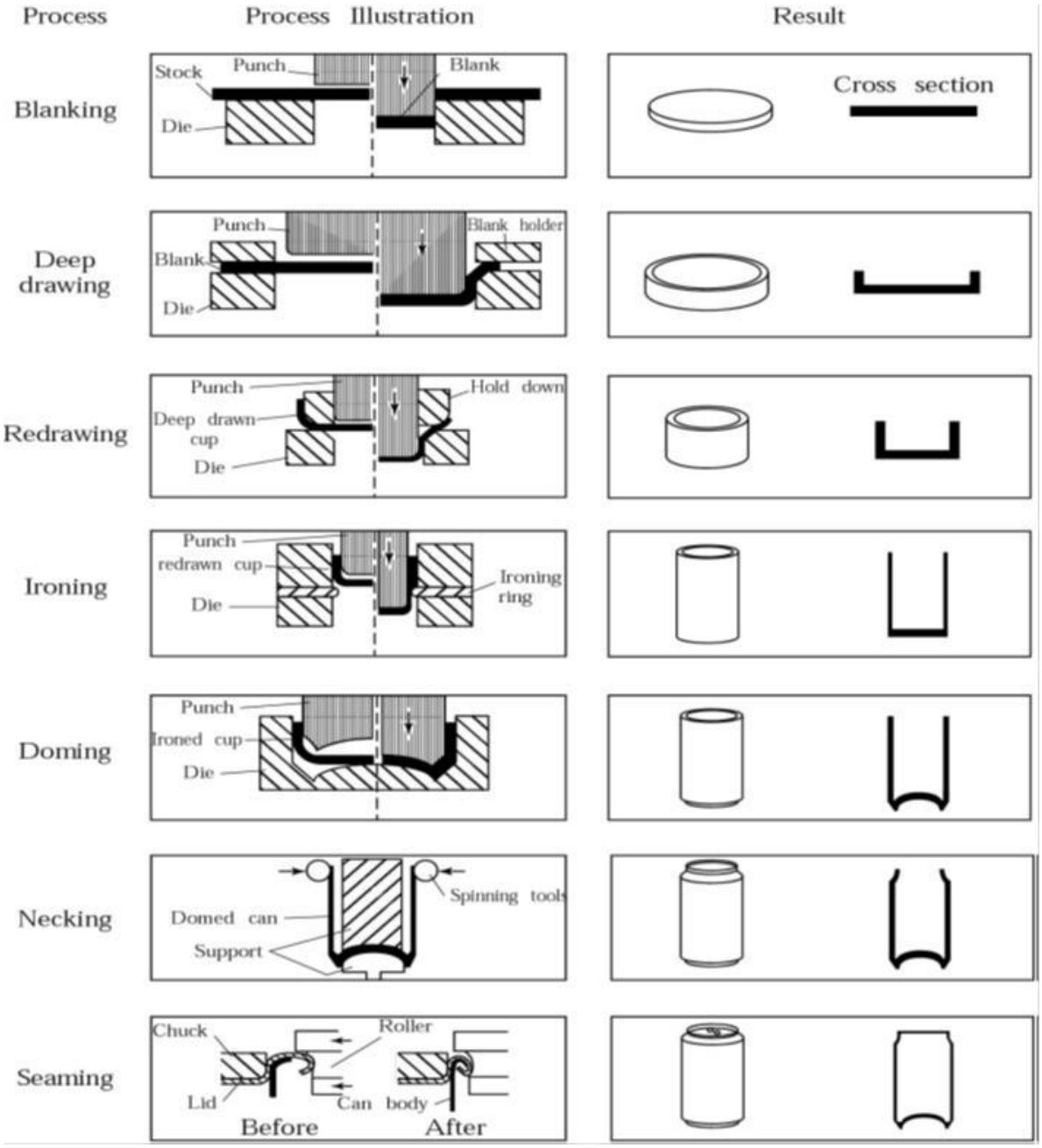

Figure 5: The metal-forming processes involved in the manufacturing a two-piece beverage can (Source: Kalpakjian.S, Schmid.S.R., Manufacturing Engineering and Technology, 2006, 4th Edi, Pearson Edu.)

5. Literature Review

5.1 Tensile properties; stress strain curve

The mechanical properties of the material in tension are obtained using standard load elongation standard test (ASTM E8). The engineering tension is widely used to provide basic design information on the strength of material and as an acceptance test for the specification of the materials. In tensile test, a specimen is subjected to a continually increasing uniaxial tensile force while simultaneous observations are made of the elongation of the specimen. The shape and magnitude of the stress-strain curve of a metal will depend on its composition, heat treatment, prior history of plastic deformation, and the strain rate and state of stress imposed during the testing (Figure 6).

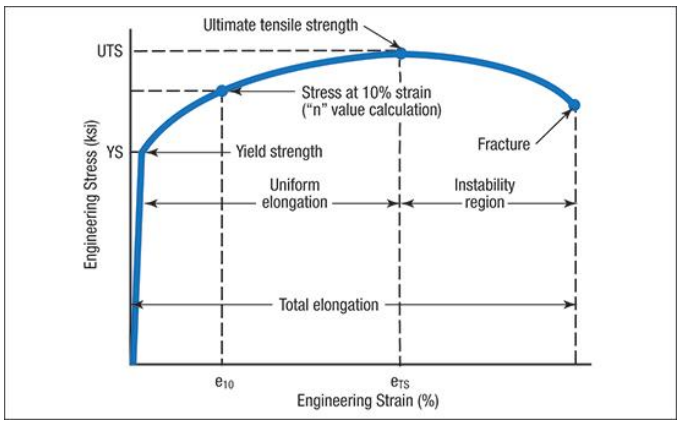

Figure 6: Typical engineering stress – strain curve
(Source: http://www.metalformingmagazine.com/magazine/article.asp?aid=9277)

In the elastic region stress is linearly proportional to strain. When the load exceeds a value corresponding to the yield strength, the specimen undergoes a plastic deformation. After this point, the stress to produce continued plastic deformation increases with increasing plastic strain i.e. the metal strain-hardens. Eventually a point is reached where the decrease in specimen cross-sectional area is greater than the increase in deformation load arising from strain hardening. The actual load required to deform the specimen falls off and the engineering stress continues to decrease until fracture occurs.

However the engineering stress-strain curve does not give a true indication of the deformation characteristics of a metal because it is based entirely on the original dimensions of the specimen, and these dimensions change continuously during the test. Because the cross-sectional area of the specimen is decreasing rapidly during necking, the load required to continue deformation falls off. The average stress based on original area likewise decreases, and this produces the fall-off in the stress-strain curve beyond the point of maximum load. Actually, the metal continues to strain-harden all the way up to fracture, so that the stress required to produce further deformation should also increase. If the true stress, based on the instantaneous measurement, the curve which is obtained is known as a true stress – true strain curve. This is also known as flow curve since it represents the basic plastic flow characteristic of the material. The relationship between engineering stress and true stress can be given by following equations.

$$\sigma = s(1 + e)$$

$$\varepsilon = \ln(1 + e)$$

Where s = engineering stress, e= engineering strain, σ = true stress, ε = true strain.

5.2 Important material parameters which affect formability

Several researchers have attempted to study the influence of material parameters on the forming characterization of a sheet metal. The important properties which are considered to influence formability significantly are yield strength, ultimate tensile strength, thickness, strength constant; strain hardening exponent, plastic strain ratio and anisotropy (Table 1).

5.2.1 Strain hardening exponent

Strain hardening exponent is one of the most important factors affecting formability. Strain hardening exponent indicates the ability of a material to distribute strain uniformly when stretched in tension. Assuming that the material is plastically isotropic and can be represented by a Holloman power-law hardening model which is given by:

$$\sigma = K\varepsilon^n$$

Where K is strength constant, ε is true strain and n is the strain hardening exponent.

Low and Garofalo, 1947, have reported the value of n for low carbon steels (0.05%C, and SAE 4340, both in annealed conditions) to be 0.26 and 0.15 respectively and the value of K to be 77000 psi and 93000 psi respectively. The strain hardening exponent may have values from n = 0 (perfectly plastic solid) to n = 1 (elastic solid) (Ducan 1967). For most of the metals n has values between 0.10and 0.50. It has large influence on the right hand side of the FLD. The forming limit in plane strain increases with increase in strain hardening exponent n. If n is reduced (by cold working) then the biaxial tension region becomes very small. Thus cold working reduces the n value and hence reduces the formability.

5.2.2 Anisotropy

Anisotropy is related to the crystallographic texture of a material's microstructure after it has under gone processing (e.g., rolling or annealing). It is a measure of the preferred grain orientations in the material and how they react under deformation. It can be represented as either normal or planar anisotropy. The normal anisotropy ($\bar{R}$) influences drawability of the sheets and planar anisotropy (Δ R) influences the wrinkling limit [Narayanasamy et al., 2008] and earing behaviour in deep drawing. Normal anisotropy measures a material's ability to resist thinning during a uniaxial tension test using the Lankford parameter:

The plastic strain ratio is defined as R = ε w / ε t

R value of a sheet is the ratio of width to thickness strain in tensile tests. The R value of drawing quality steel is 1.2-2.0 and that of aluminium sheets is usually less than 1.

5.2.3 Thickness

Higher forming limits are found for thicker sheets. Higher limit strains may be attributed to larger necking zones due to higher thickness [Feliksstachowicz, 1986].The cross section of neck is geometrically similar in thick and thin sheets of the same material. These neck shapes depends on the rate sensitivity (m) of the material.

Table 1: Sheet metal characteristics and their importance (Source: Kalpakjian.S, Schmid.S.R., Manufacturing Engineering and Technology, 2006, 4th Edi, Pearson Edu.)

Characteristic	Importance
Elongation	Determines the capability of the sheet metal to stretch without necking and failure; high strain-hardening exponent (n)and strain-rate sensitivity exponent (m)desirable.
Yield-point elongation	Observed with mild-steel sheets; also called Lueder's bands and stretcher strains; causes flamelike depressions on the sheet surfaces; can be eliminated by temper rolling, but sheet must be formed within a certain time after rolling.
Anisotropy (planar)	Exhibits different behavior in different planar directions; present in cold-rolled sheets because of preferred orientation or mechanical fibering; causes earing in drawing; can be reduced or eliminated by annealing but at lowered strength.
Anisotropy (normal)	Determines thinning behavior of sheet metals during stretching; important in deep-drawing operations.
Grain size	Determines surface roughness on stretched sheet metal; the coarser the grain, the rougher the appearance (orange peel); also affects material strength.
Residual stresses	Caused by nonuniform deformation during forming; causes part distortion when sectioned and can lead to stress-corrosion cracking; reduced or eliminated by stress relieving.
Springback	Caused by elastic recovery of the plastically deformed sheet after unloading; causes distortion of part and loss of dimensional accuracy; can be controlled by techniques such as overbending and bottoming of the punch.
Wrinkling	Caused by compressive stresses in the plane of the sheet; can be objectionable or can be useful in imparting stiffness to parts; can be controlled by proper tool and die design.
Quality of sheared edges	Depends on process used; edges can be rough, not square, and contain cracks, residual stresses, and a work-hardened layer, which are all detrimental to the formability of the sheet; quality can be improved by control of clearance, tool and die design, fine blanking, shaving, and lubrication.
Surface condition of sheet	Depends on rolling practice; important in sheet forming as it can cause tearing and poor

5.3 Microstructure

The study of microstructure is a part of metallography. Metallography is the study of microscopic structure of metal and alloys using microscope. The study of microstructure is useful in understanding the performance and reliability of metal and alloys. In addition, it is helpful in material development, inspection of incoming material, manufacturing control and failure analysis. Metallography or microstructural analysis includes, but is not limited to, the analysis of grain size, porosity and voids, phase analysis, dendritic growth, cracks and other defects, corrosion analysis, inter-granular attack (IGA), coating thickness and integrity, weld and heat-affected zones (HAZ), etc. (Metallographic handbook, 2011).

5.4 Forming Limit Diagram (FLD)

Forming Limit Diagram (FLD) is a useful technique for controlling failure in sheet metal forming. It gives an indication whether the material can sustain certain ratio of strains without failure. The use of grid of circles for accessing the formability of sheet metal was pioneered by Keeler (Keerler, 1965) and Goodwin (Goodwin 1968). It is a graphical representation of limit strain subjected to different load condition.

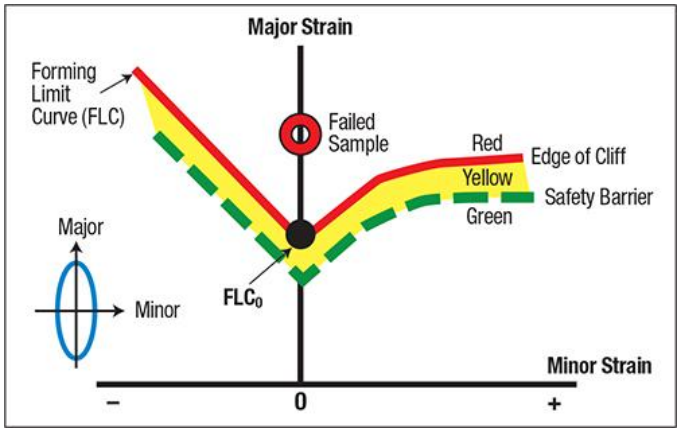

Figure 7: Typical forming limit diagram (source: metal forming magazine, 2015)

The experimental determination of FLD consist of printing a grid of circles of appropriate diameter (In the present study, 2.5 mm diameter is used) on the surface of sheet. The printing of circular grid is advantageous as the circles will get deformed into ellipses with their major and minor axes directed along the principal direction of strain. Principal strain can be determined by measuring the axes of ellipse and diameter of original circle. The major and minor axes of an ellipse represent the two principal strain directions. The strains obtained from above procedure are used to determine failure. As discussed above various factors affecting the FLD diagram, are highlighted below also

- Material properties – strain hardening and strain rate exponent
- Thickness of sheet
- Anisotropy in the sheet
- The forming limit curve of softened sheet of the same alloy and same thickness is positioned higher to that of hard sheet
- Type of coating on the sheet
- Type of pre-straining prior to testing
- Orientation of test specimen with respect to rolling direction

5.5 Finite Element Analysis

The FE simulation was performed in DYNAFORM software to check the accuracy of failure obtained in stretch forming experiment. The FE simulation was carried out in DYNAFORM 5.8, commercially available dedicated software for sheet metal forming applications. This system provides pre-processing (auto meshing, tool positioning, draw bead representation) and post-processing (animation, formability plot, forming limit diagram). The DYNAFORM uses LS DYNA (an explicit time integration dynamic solver) in conjunction with the pre-processor and the LS-POST post processor. The failure predictions based on the developed as well as existing correlations were compared with the experimental results. The tools and the blank are modelled and meshed in a pre-processor and analysis is carried out on a solver. The results are viewed and analysed in a post processor.

6. Material and methods

6.1 Material specification

Stainless (SS) 202 material was selected for the current study due to it's increasingly popularity for structural and non-structural application. These SS 200 series sheets are widely used for utensil and cutlery manufacturing in India and abroad (Figure 8). The main advantage of using these sheets for utensil manufacturing is its low cost in comparison with SS 300 series.

Figure 8: Utensils manufactured from SS sheets (ISSF, New 200 series steel, 2005)

As discussed above, 16 SWG (Standard Wire Gauge) sheets which is a raw material to the company is first reduced to 20 SWG by rolling after performing annealing and pickling processes. Similarly 20 SWG is reduced to 22 SWG. The SS sheets of all three gauges viz. 16

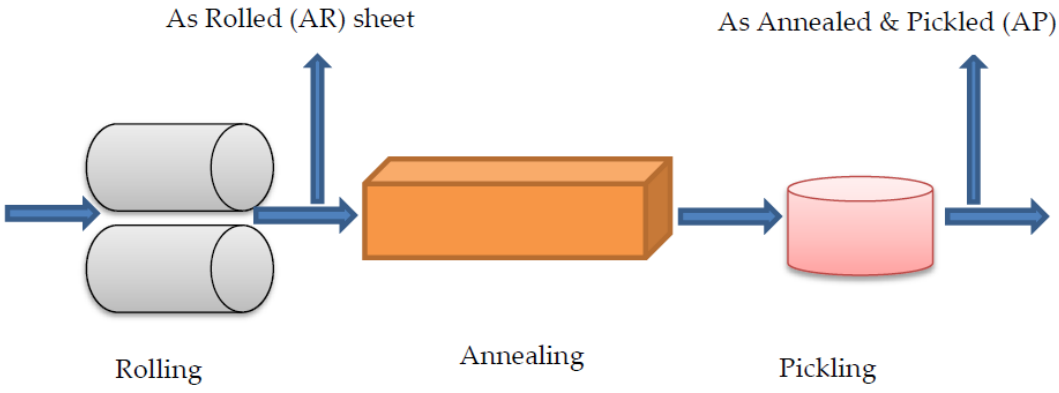

Figure 9: Specimen used for formability characterization

SWG, 20 SWG and 22 SWG of both As Rolled (AR) and As Annealed & Pickled (AP) were arranged for formability characterization from Monika Udyog, Ahmedabad (Figure 9).

6.2 Chemical composition of materials

The chemical compositions of materials used in the present work have been analysed by spectroscopy are given in Table 2.

Table 2: Chemical composition of the SS 200 series by spectroscopy (ASTM E – 1086 – 2008)

ASTM-E-1086 (Spectroscopy)									
Gauge/element (%)	C	Si	S	Po	Mn	Ni	Cr	Mo	Cu
16 SWG	0.078	0.350	0.011	0.058	9.4	0.350	12.73	0.053	1.55
20 SWG	0.078	0.370	0.010	0.058	9.43	0.3	12.7	0.052	1.54
22 SWG	0.098	0.4	0.008	0.049	9.22	0.250	12.33	0.016	1.5

It can observe from the table that these grades of sheets have low nickel content.

6.3 Test methods: Tensile properties

6.3.1 Determination of tensile properties

Instron uniaxial tension machine installed at Plasticity and Metal Forming (PMF) lab at Delhi Technological University (DTU), Delhi was used for carrying-out tensile test of the As Annealed & Pickled (AP) specimens (Figure 10). The As Rolled (AR) specimens were tested in Material Test System (MTS, 800) machine installed at Naval Defence Research (NDR) Lab at Indian Institute of Technology (IIT), Delhi (Figure 11). The standard tensile properties such as yield stress, ultimate tensile stress, uniform elongation and total elongation was determined from the stress- strain data.

Figure 10: Instron uniaxial testing m/c at DTU

Figure 11: MTS, 800 m/c in NDR lab at IITD

The specimens as per ASTM standard E8M as shown in Figure 12 and Figure 13 were used for tensile testing. The specimens were prepared by laser cutting in three directions with the length parallel (00), diagonal (450) and perpendicular (900) to the rolling direction of the sheet.

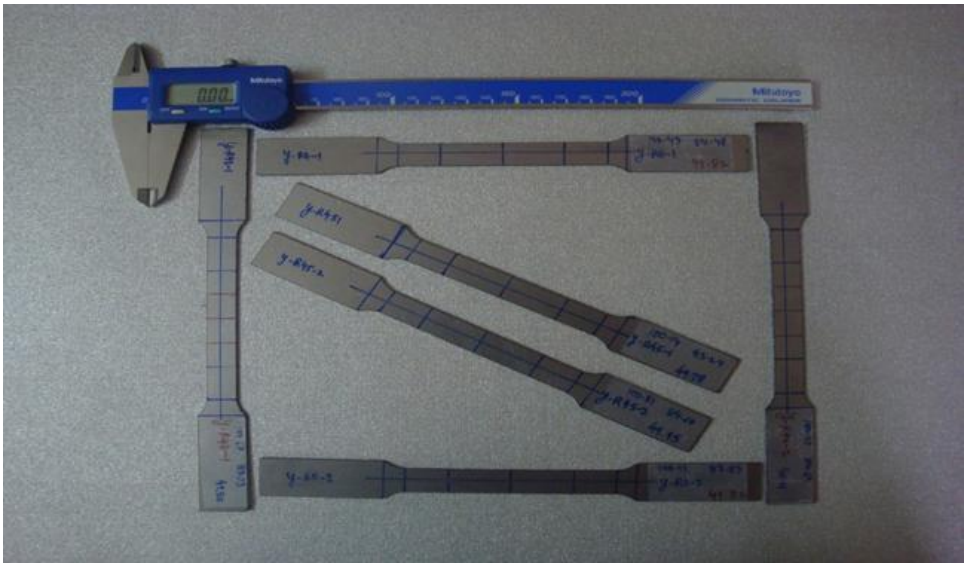

Figure 12: Specimen as per the ASTM standard E8M

Load elongation data was obtained for all the tests which were converted into engineering stress strain curves. The point corresponding to max stress was taken as the UTS and the stress at 0.2% offset was taken as the YS. The total elongation was measured using an initial gauge length of 50mm.The strain hardening behaviour can be described using the Holloman's equation.

$$\sigma = K\varepsilon^n$$

Where σ=true stress, ε=true strain, n=strain hardening exponent, K=strength coefficient.

For determining the n value of these sheets, the engineering stress strain data were converted into true stress-true strain curves using the following equations.

$$\sigma = s(1 + e)$$

$$\varepsilon = \ln(1 + e)$$

Where s = engineering stress and e= engineering strain.

The log true stress and log true strain values were calculated in the uniform plastic deformation range (between YS and UTS) and using linear regression (least square method) a best fit was plotted. The slope of this line gives n value and Y- intercept gives log K. The strain hardening was observed to be occurring throughout the tensile test but broadly in three stages. In the stage-1, rate of strain hardening is low, stage-2 is characterised by a dip in the rate of strain hardening and the stage-3 was observed with accelerated strain hardening till fracture. The final strain hardening exponent was evaluated by taking average of all three stages. (Gautam, V. 2014)

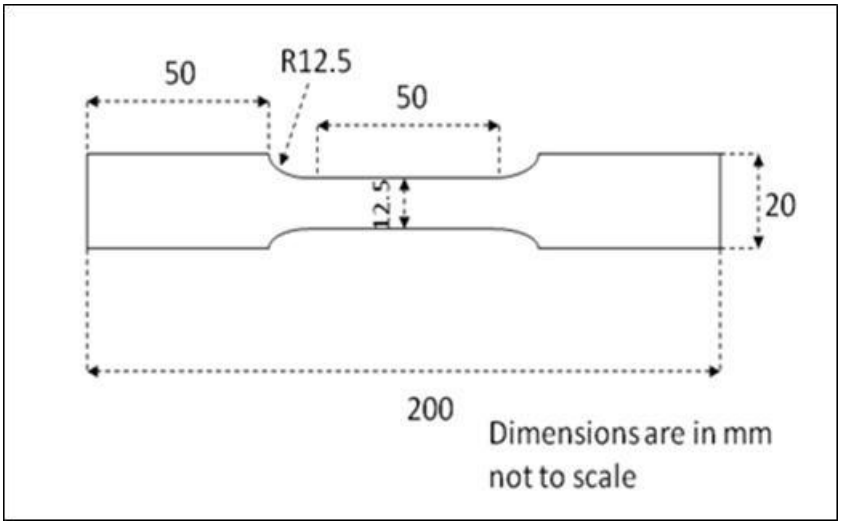

Figure 13: Dimensions of Tensile specimen (ASTM E8)

6.3.2 Determination of average plastic strain ratio (Normal anisotropy – Ravg value)

The plastic strain ratio, which is a measure of anisotropy, would be determined using specimens prepared according to ASTME517 specification. Final width and gauge length would be measured and the plastic strain ratio (R) would be calculated as below [George E Dieter, Mechanical metallurgy].

$$\boldsymbol{R = \frac{\varepsilon_w}{\varepsilon_t} = \frac{\varepsilon_w}{-(\varepsilon_w + \varepsilon_l)} = \frac{\ln \frac{w_f}{w_0}}{\ln \frac{l_0 w_0}{l_f w_f}}}$$

W_0, l_0: initial width and length, W_f, l_f: final width and length

Ɛw=true width strain

Ɛt=true thickness strain

Ɛl=true length strain

The R value would be determined in three directions as mentioned in the tensile tests by repeating the above procedure. The normal anisotropy or average plastic strain ratio would be calculated using the formula:

$$Ravg = (R_0+R_{90}+2R_{45})/4$$

R_0, R_{45} and R_{90} represent the R value in three directions.

6.3.3 Sample preparation

Samples as per ASTM E8 standard for the determination of tensile properties and anisotropic parameter were prepared using lazer cutting (Laser TLF 400o Turbo, Make: TRUMPF, Model: LC 3030 111909) technique locally at Rishi Lazer Ltd, Kundli, Distt. Sonepat, Haryana (Figure 14).

Figure 14: Specimen cutting using Lazer machine

Multiple samples from sheets (AISI 202 Stainless steel) of all three available thickness viz. 16 SWG (~1.4 mm), 20 SWG (~0.84mm) and 22 SWG (~0.6 mm), of both AP and AR specimens were prepared by lazer cutting at an angle 0^O (Parallel), 45^O (Diagonal) and 90^O (Perpendicular) to the rolling direction of the sheet (Figure 15). This was mainly done to find out anisotropic property as well as to understand tensile behaviour across above angles.

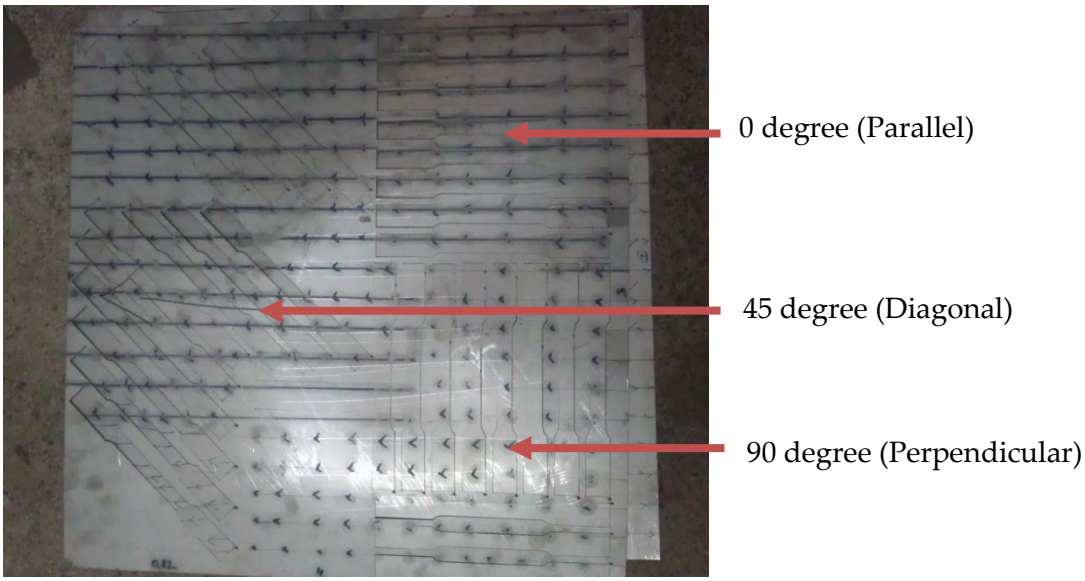

Figure 15: Cutting pattern of specimens in 0^o, 45^o, 90^o to the rolling direction

6.3.4 Sample selection

In order to gain the accuracy of results, a total of three samples of each rolling direction viz. parallel, diagonal and perpendicular of each available thickness viz. 16 SWG (~1.4 mm), 20 SWG (~0.84mm) and 22 SWG (~0.6 mm), for both AR and AP specimens were tested (Figure 16). To this effect, a total of about 30-35 samples each of AR and AP specimens were tested and out of which results of duplicate specimens were included in the following discussions.

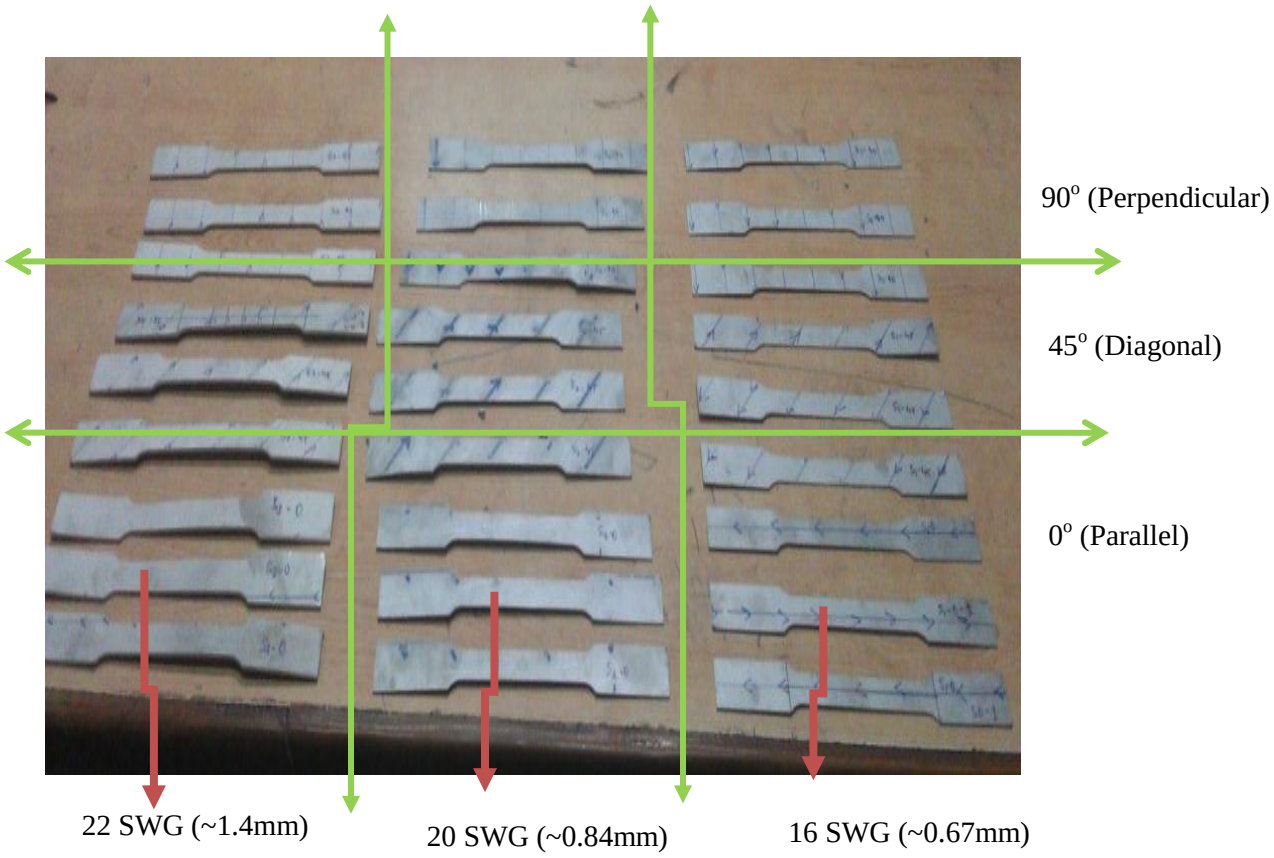

Figure 16: Specimens tested during tensile testing

Samples were designated as S(1 or 2 or 3)-(0 or 45 or 90)-(1 or 2)-AR or AP which symbolizes (sample gauge; 1 indicate 22 SWG, 2 indicate 20 SWG, 3 indicate 16 SWG)-(Rolling direction; 0 indicate parallel to rolling direction, 45 indicate diagonal to rolling direction, 90 indicate perpendicular to rolling direction)-(Number of samples)

Table 3: Specimen designation methodology

Gauge details			**Rolling direction**			**Specimen number**		**AR or AP**	
S1	S2	S3	0	45	90	1	2	AR	AP
22 SWG (0.6 mm)	20 SWG (0.8)	16 SWG (1.4)	Parallel	Diagonal	Perpendicular	Specimen 1	Specimen 2	As Rolled	Annealed & Pickled

6.4 Microstructure

6.4.1 Sample preparation

The samples for the microstructure observation were prepared at metallurgical lab at DTU. As a first step, the samples of each gauge (thickness) viz 16 SWG (1.4 mm), 20 SWG (0.8 mm) and 22 SWG (0.6 mm) of both AR and AP were cut and mounted. Mounting of the samples were done with the help of acrylic castable mounting using a frame (Figure 17). After initial mounting the samples were left overnight for solidifying and drying.

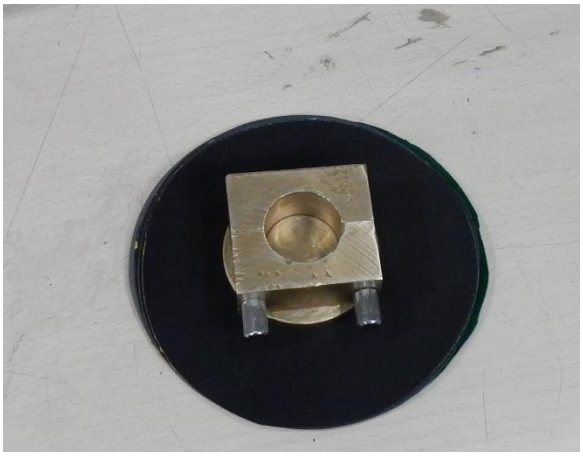

Figure 17: Frame used for mounting samples

After the samples were solidified, these were polished using series of different grade of emery papers starting with coarse grains to progressively fine grain (2000, 1200, 1000, 800, 600, 400, 220 grits) (Figure 18).

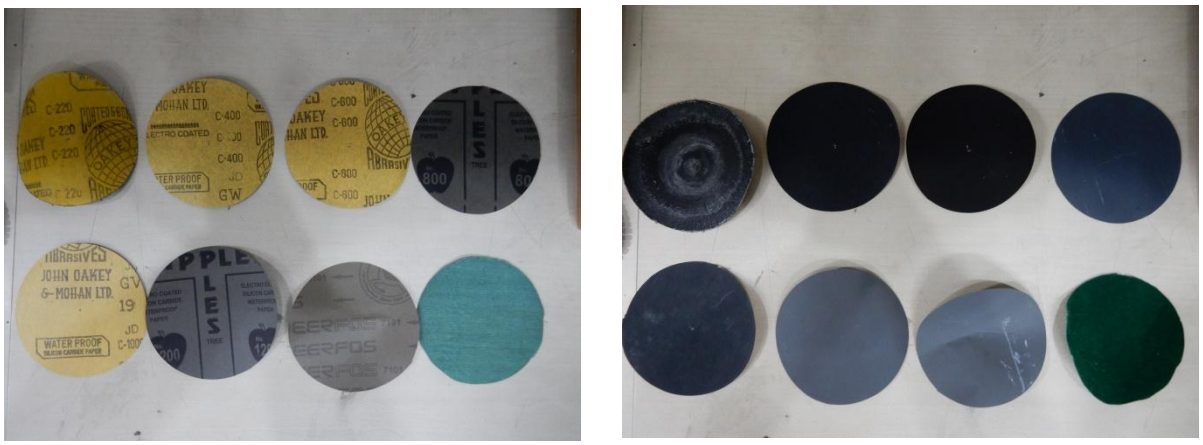

Figure 18: Emery paper used for polishing samples

After the samples were given coarse polishing, the samples were fine polished on rotating disc with alumina powder (Figure 19).

Figure 19: Fine polishing step

In the final stage, the samples were etched using 1ml Hydrochloric acid, 3ml Nitric acid and 1 ml Glycerol with impression time of about 10 seconds (Sudhakaran, et. Al 2014).

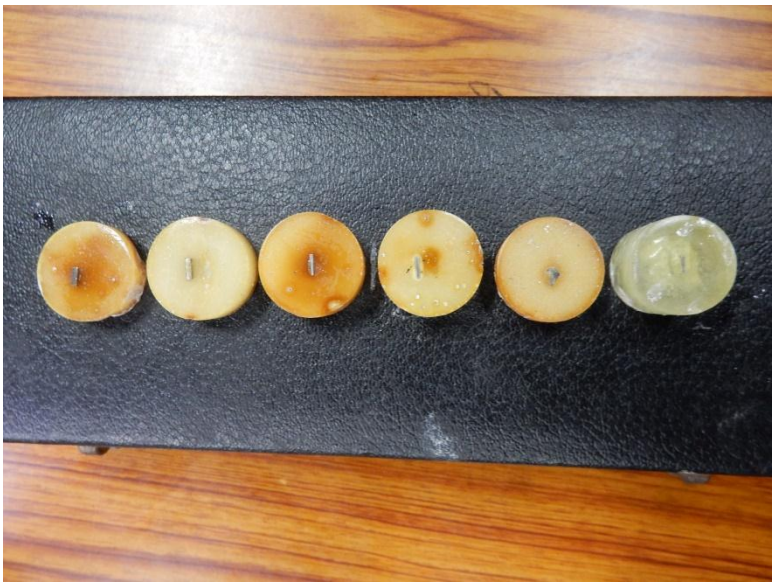

Figure 20: Samples for microstructure observation

6.4.2 Microstructure observation

Microstructures of the samples were observed in the OLYMPUS-MI optical microscope (Olympus Opto Systems India Private Limited) installed at metallurgy lab at DTU. This microscope is equipped with the image analysis software, a camera and a computer.

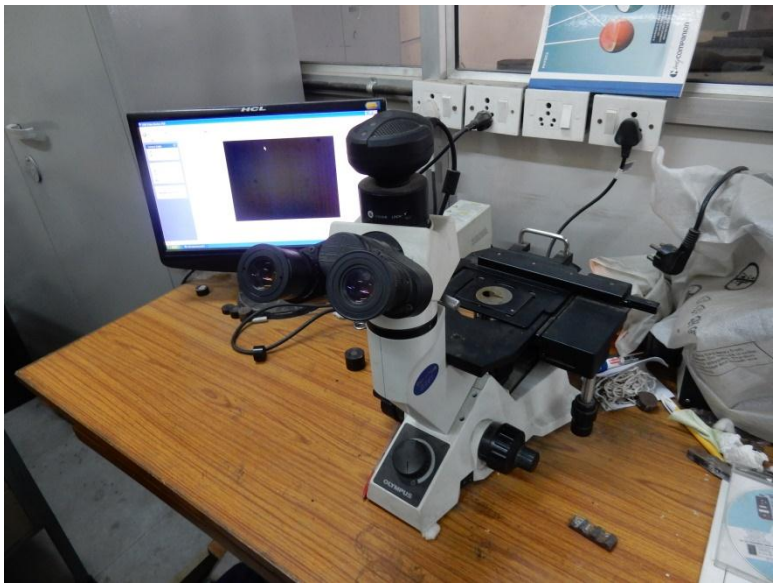

Figure 21: Setup for microstructure observation

6.5 Forming Limit Diagram (FLD)

6.5.1 Specimen preparation

The specimen of 22 gauge of AP was selected for FLD analysis. The objective was to get an experimental determination of FLD and verify the same using Finite Element Analysis (FEA). The prime motivation for selecting 22 gauge AP specimens was that these sheets are finally used for making utensil manufacturing by various end customers.

As a starting step, the grid of circles was marked on the specimens by lazer marking machine. The diameter of the circle marked on the specimens for the present study was 2.5 mm (Figure 22).

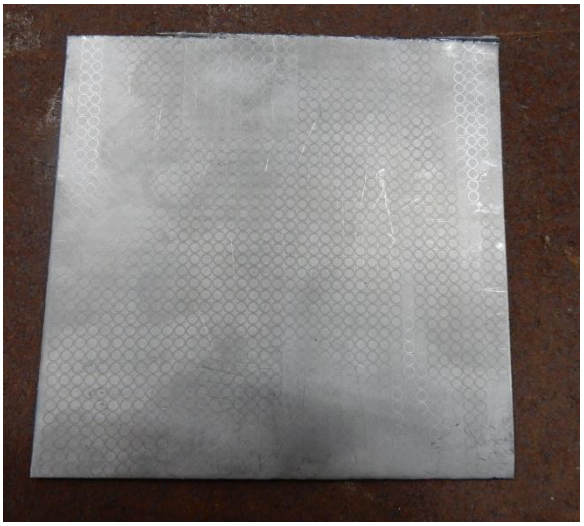

Figure 22: Grid of circles marked on the specimen sheet

After the grid of circles were marked, the rectangular specimens of size 100 mm x 100 mm, 100 mm x 80 mm, 100mm x 60mm, 100mm x 40mm, 100mm x 20 mm were cut for formability test. The rectangular specimens were cut in the shearing machine installed at central workshop at IIT, Delhi (Figure 23).

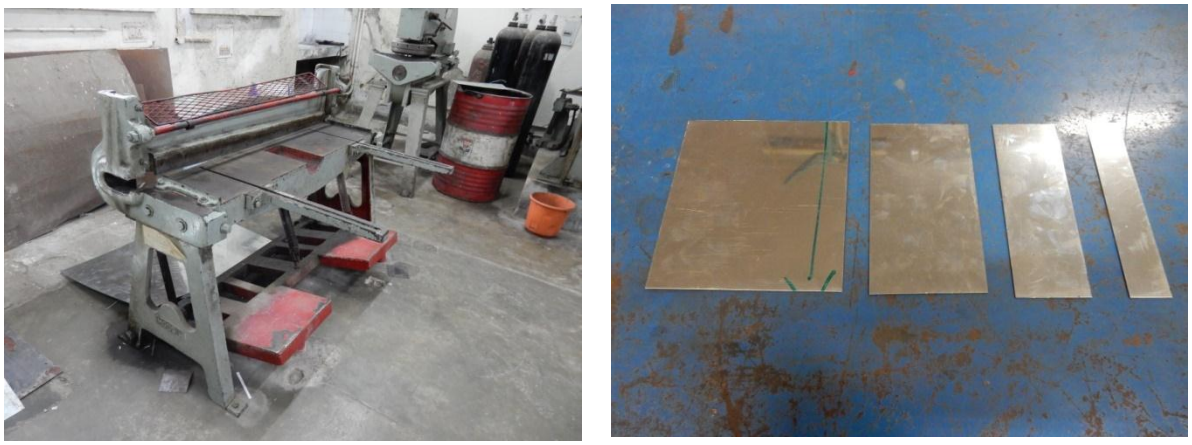

Figure 23: Shearing m/c used and photo of specimens

6.5.2 Stretch forming experiment

The prepared specimens were tested for stretch forming experiments in a 100 tonne hydraulic press installed at Central Workshop at Indian Institute of Technology (IIT), Delhi. The specimens were placed between the upper die and lower die. An optimum blank holding force was applied to clamp the specimens. A mirror was used to observe the necking or deformation of the specimens. Experimental setup used for performing the stretch forming experiment is depicted in Figure 24.

Figure 24: Stretch forming experimental setup

While performing the experiments in the hydraulic press, it was observed that the specimens used in the present study were cracking at once without necking (Figure 25).

Figure 25: Specimens cracked during the experiments

To this effect, the forming experiments were performed till just before the cracking based on the personal observation. The experiments of the remaining specimens were conducted in the safe condition i.e. just before crack (Figure 26).

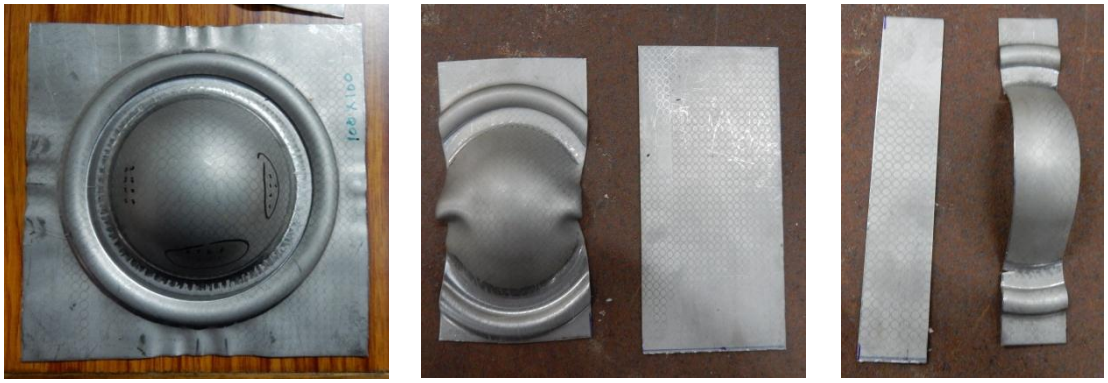

Figure 26: Specimens before and after forming experiments

6.5.3 Strain measurement

The strain measurement was done in travelling microscope (Radical make, model no – IS500, least count – 0.001mm) installed at PMF lab at Delhi Technological University (DTU). Major and minor principal strains were calculated by measuring major and minor diameters of ellipses on the deformed samples. On the basis of the results obtained from the major and minor strains, forming limit diagram was plotted. A picture of travelling microscope installed at DTU is presented in Figure 27.

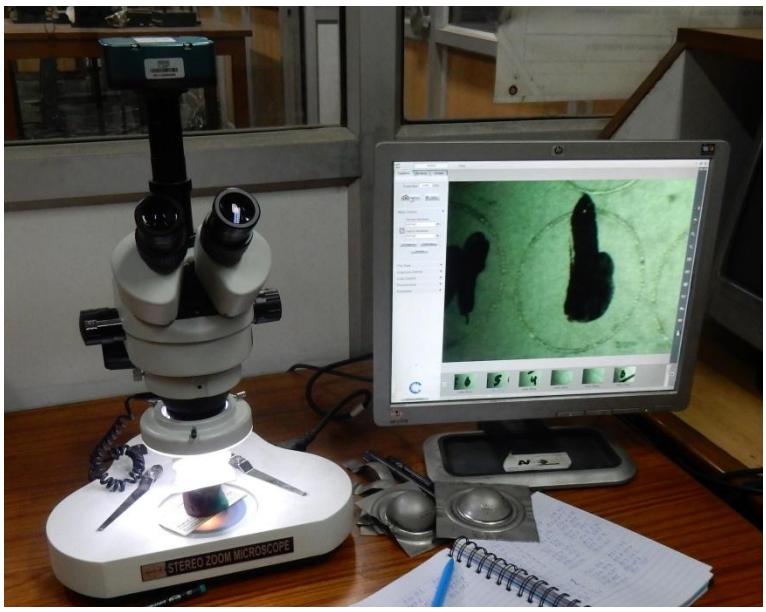

Figure 27: Travelling microscope

6.5.4 Height measurement

The dome height (LDH) of 100mm x 100mm specimen just before the point of necking/fracture was measured using a vernier height gauge with a least count of 0.02 mm (Figure 28).

Figure 28: Dome height measurement using vernier height gauge

6.5 Finite Element Analysis

The stretch forming simulations were carried out using a 50 mm hemispherical diameter punch. The dimension of blank used was 100mm X 100mm, die used was 52 mm, die corner radius was 9mm and punch corner radius was 6mm. The blank was placed at the center of the die. All tools were considered to be rigid bodies and they were meshed using 'automesh' option (Figure 29).

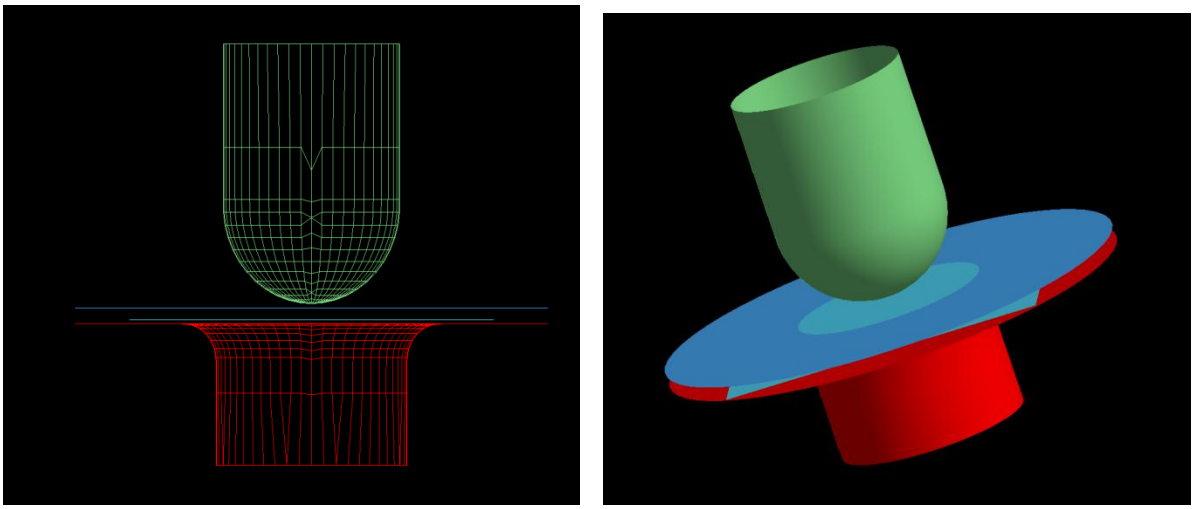

Figure 29: Mesh and solid models made in FEM

Material properties used as a feed for FEM analysis for the present study includes Punch travel as 50 mm, Blank holding force as 10000 N, Coefficient of friction as 0.125 and Punch speed as 5000 mm/sec. The experimental value of strain hardening exponent (n) and strength coefficient were provided as input for material properties (Figure 30)

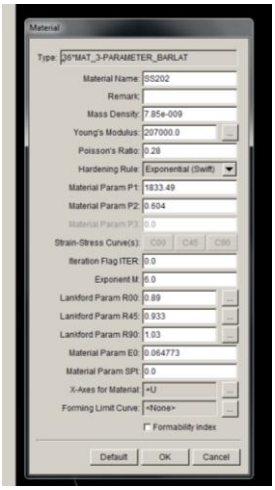

Figure 30: Material parameters used in FEA software

7. Results and discussions

7.1 Tensile properties

7.1.1 Stress strain curve of As Annealed & Pickled (AP) sheets

Typical engineering stress-engineering strain curve and a true stress-true strain curve of AP specimens of thickness gauge 22 SWG corresponding to orientation 0, 45 and 90 degree to rolling direction are shown Figure 31. Similarly 20 SWG are shown in Figure 32 and 16 SWG are shown in Figure 33.

The value of yield strength i.e. onset of permanent deformation, was taken at 0.2% engineering strain. The values of strength (YS and UTS) and ductility (% elongation) show a large variation in mechanical properties. Ultimate Tensile Strength (UTS) was determined by maximum load and original cross-section area of the specimen. The variation of UTS with the rolling direction is depicted in Figure 34. The variation of percentage elongation with the rolling direction is depicted in Figure 35. These mechanical properties do not follow any particular trend making it difficult to predict any pattern (Desu RK, 2015), however the variation in the tensile properties may be attributed to the anisotropic behaviour of stainless steel sheet (Gautam et al 2015).

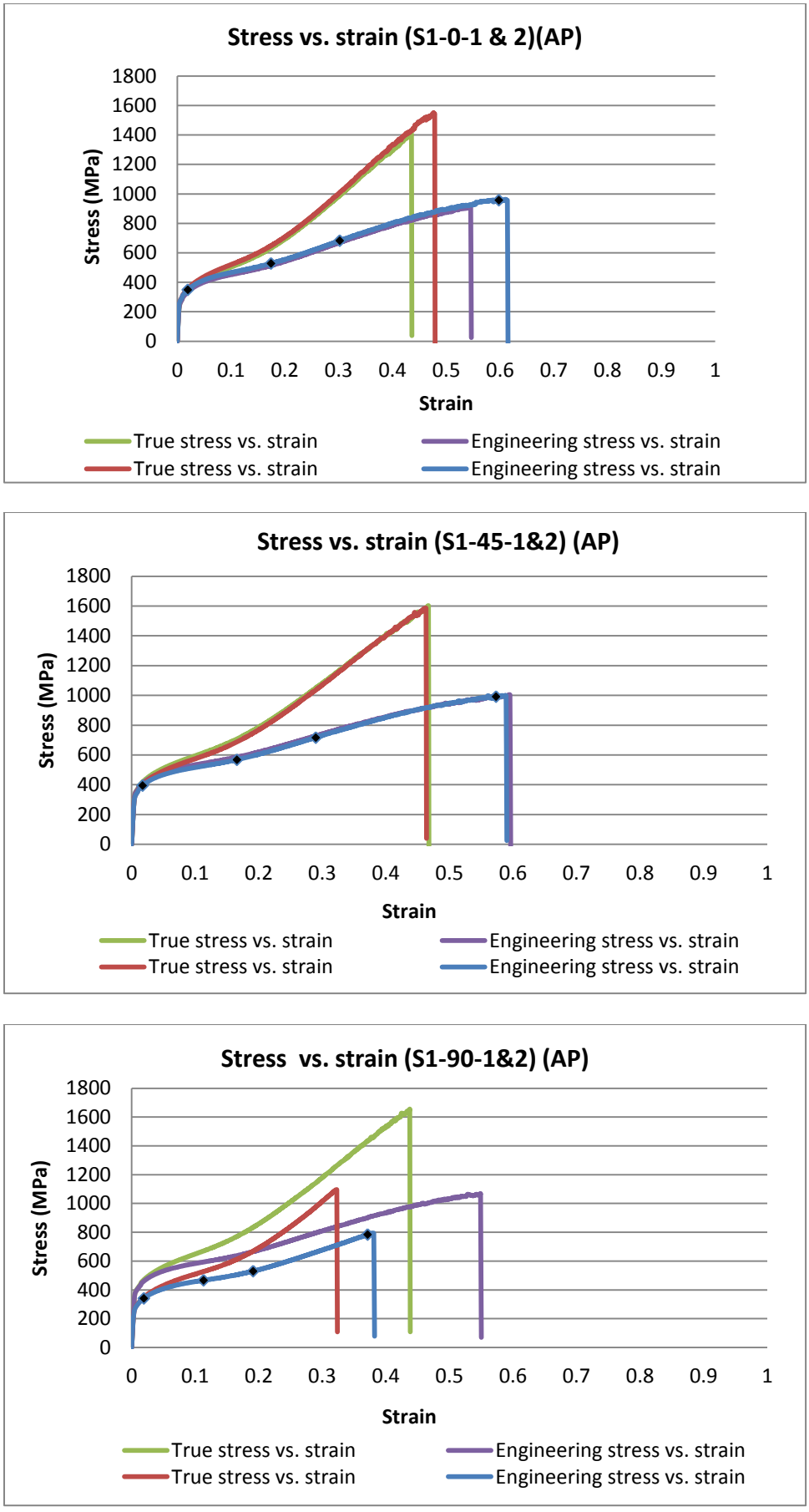

Figure 31: E. Stress vs. strain and True stress vs. strain curve of 22 SWG (0.6 mm) thickness specimen

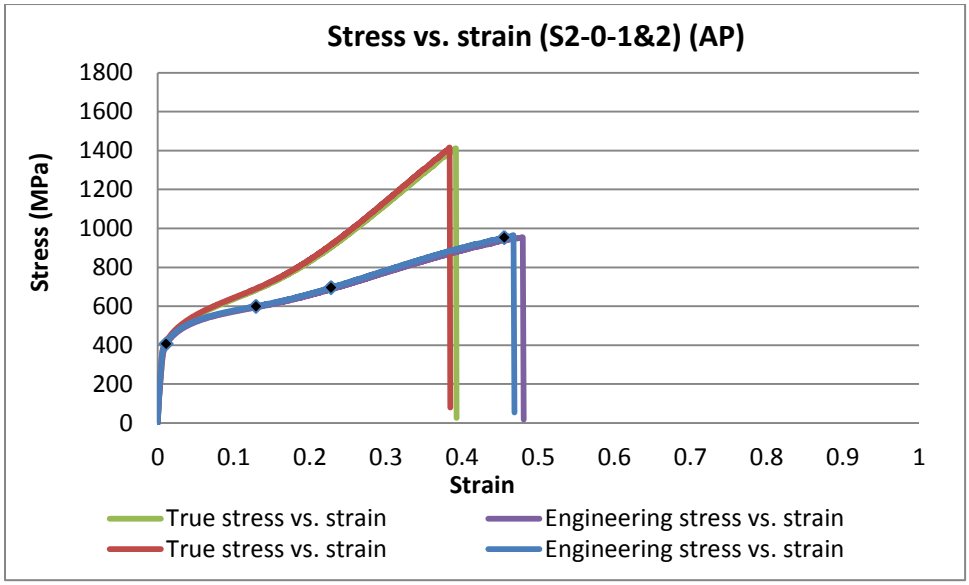

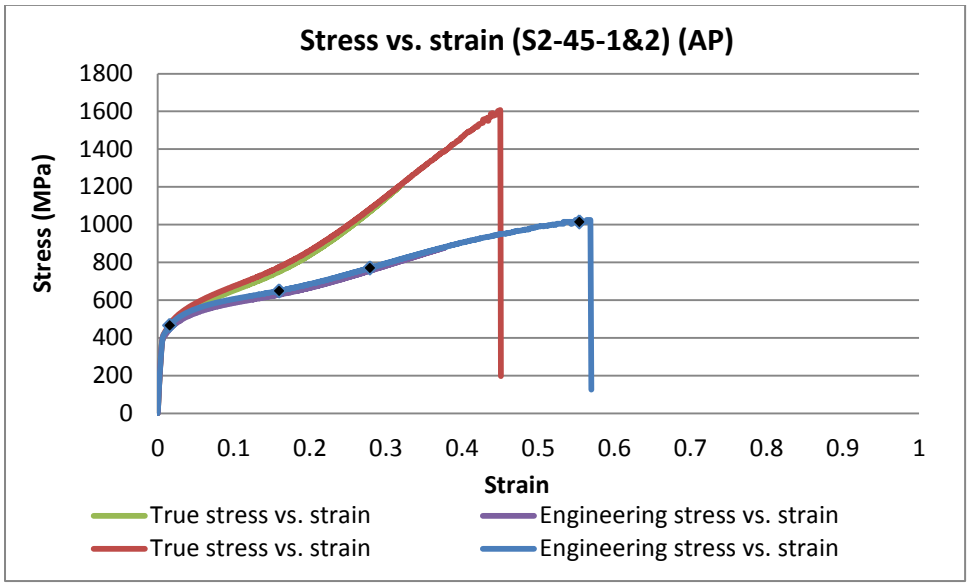

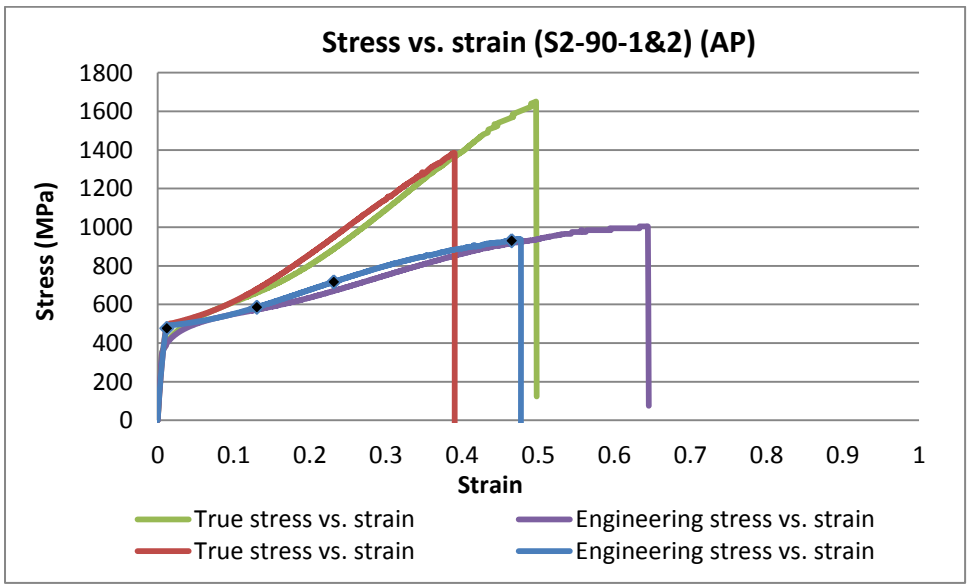

Figure 32: E. Stress vs. strain and True stress vs. strain curve of 20 SWG (0.8 mm) thickness specimen

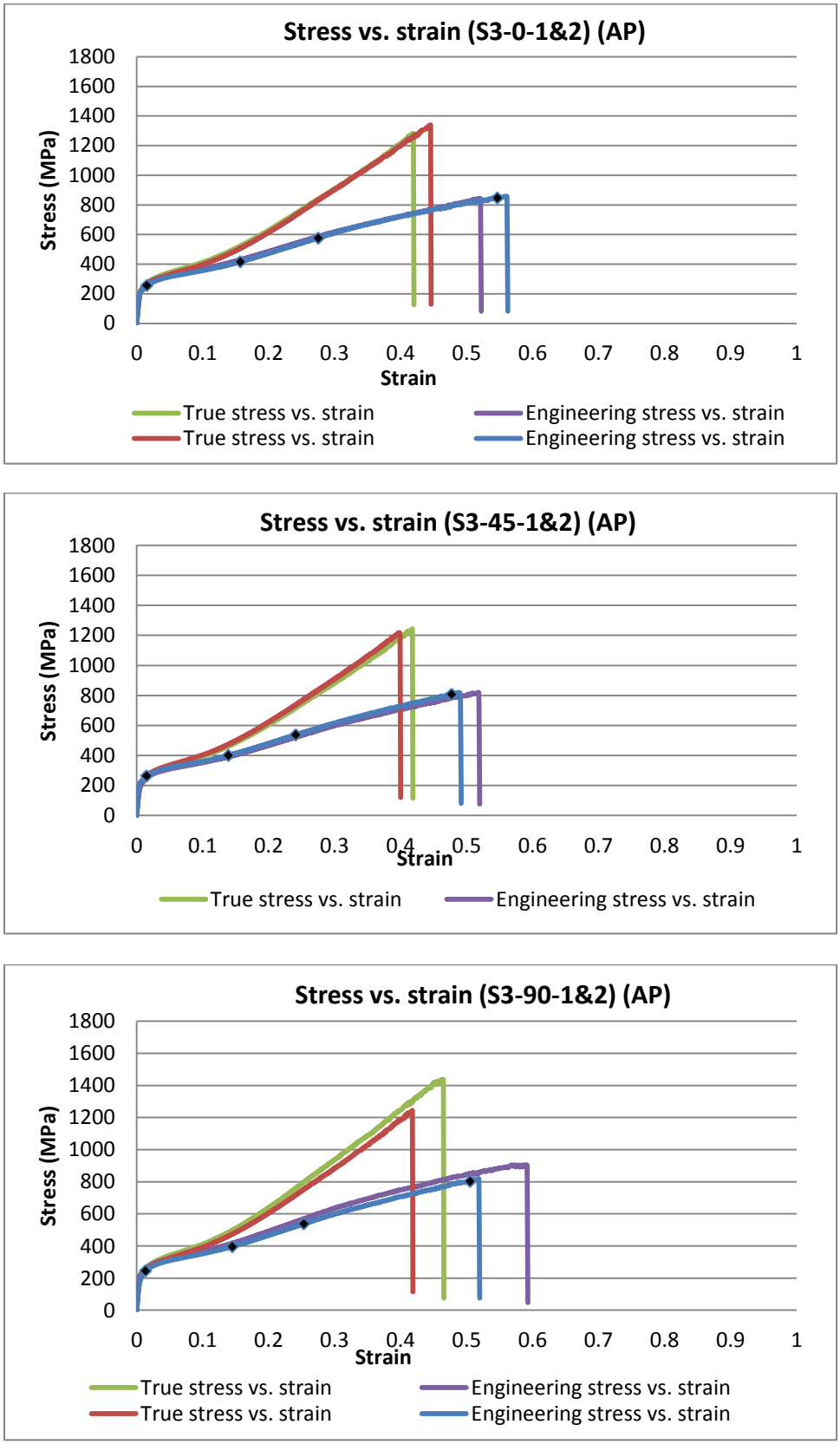

Figure 33: E. Stress vs. strain and True stress vs. strain curve of 16 SWG (1.4 mm) thickness specimen

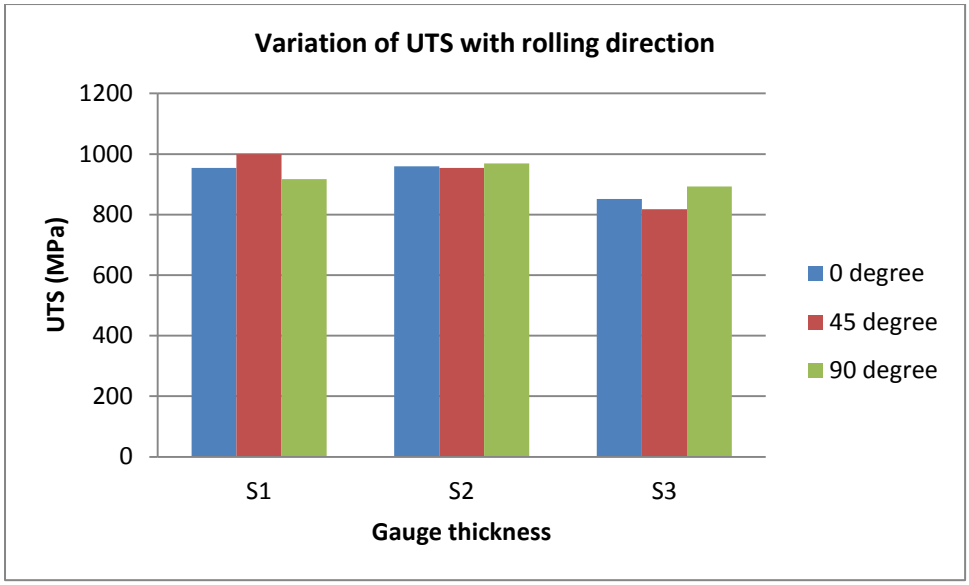

Figure 34: Variation of ultimate tensile strength (UTS) with rolling direction

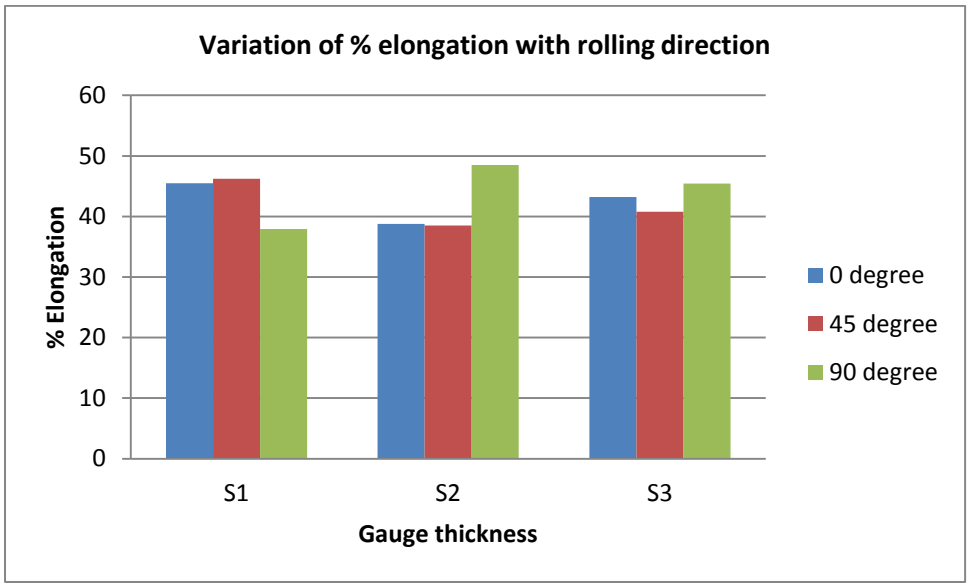

Figure 35: Variation of % elongation with rolling direction

During cold rolling of sheet metal, the material develops anisotropy. The flow strength in thickness direction becomes different to that in the plane of sheet. For testing the anisotropy, the test specimens are cut at an angle (0, 45 and 90) to rolling direction. The results of anisotropy test are compiled for normal and planar anisotropy for both individual samples and average of each thickness. The details of anisotropy results are discussed below.

7.2 Anisotropic properties of AP specimen

7.2.1 Thickness 22 SWG (~0.67 mm) specimen

The planner anisotropy of 22 SWG specimen was found to be 0.0319 and normal anisotropy was found to be 0.9767. The details of the anisotropy of specimen in the direction parallel, diagonal and perpendicular are depicted in the Figure 36.

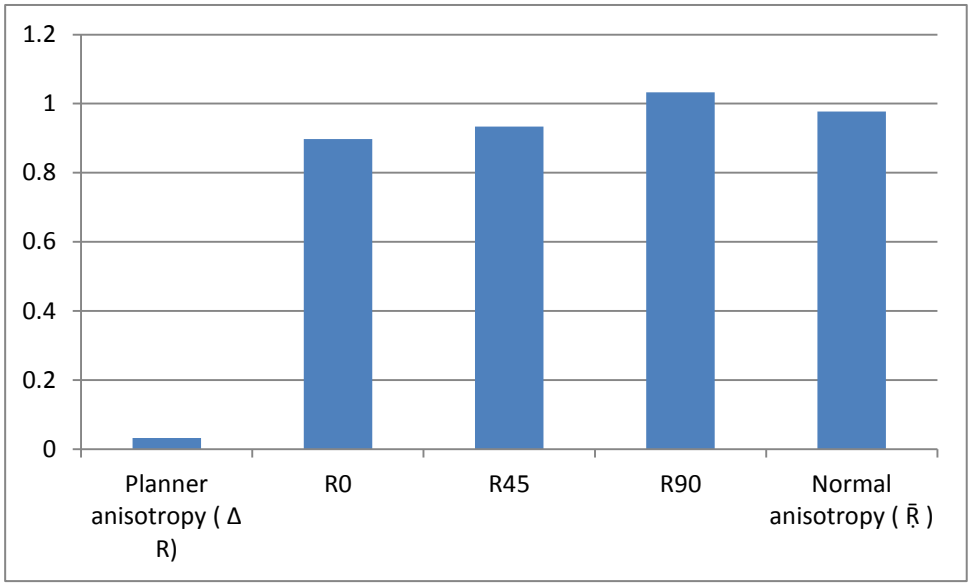

Figure 36: Comparative graphs of various anisotropic values of 22 SWG sheets

7.2.2 Thickness 20 SWG (~0.84 mm) specimen

The planner anisotropy of 20 SWG specimen was found to be -0.04157 and normal anisotropy was found to be 0.9535. The details of the anisotropy of sheet in the direction parallel, diagonal and perpendicular are depicted in the Figure 37.

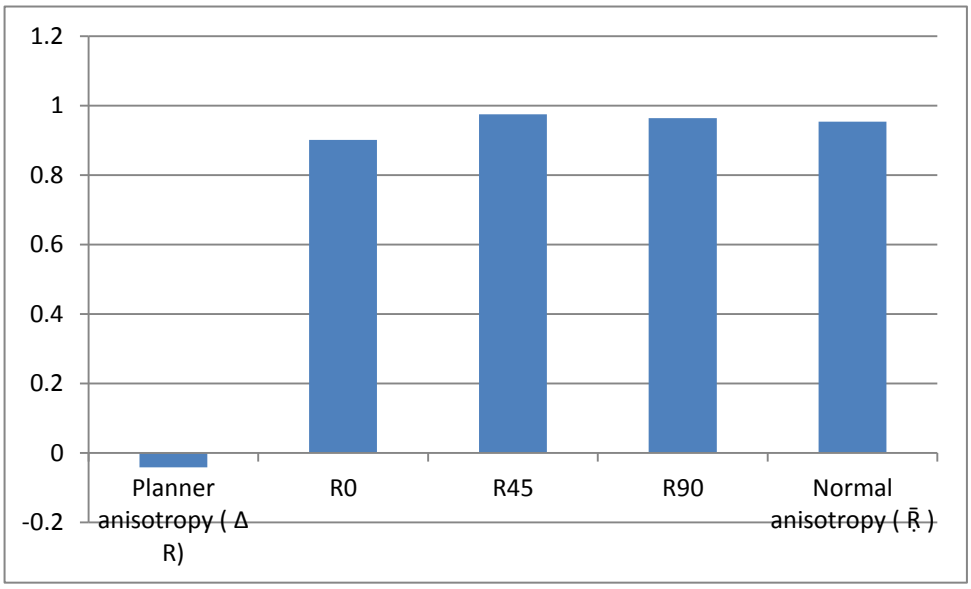

Figure 37: Comparative graphs of various anisotropic values of 20 SWG sheets

7.2.3 Thickness 16 SWG (~1.4 mm) specimen

The planner anisotropy of 16 SWG specimen was found to be 0.04915 and normal anisotropy was found to be 0.84636. The details of the anisotropy of sheet in the direction parallel, diagonal and perpendicular are depicted in the Figure 38.

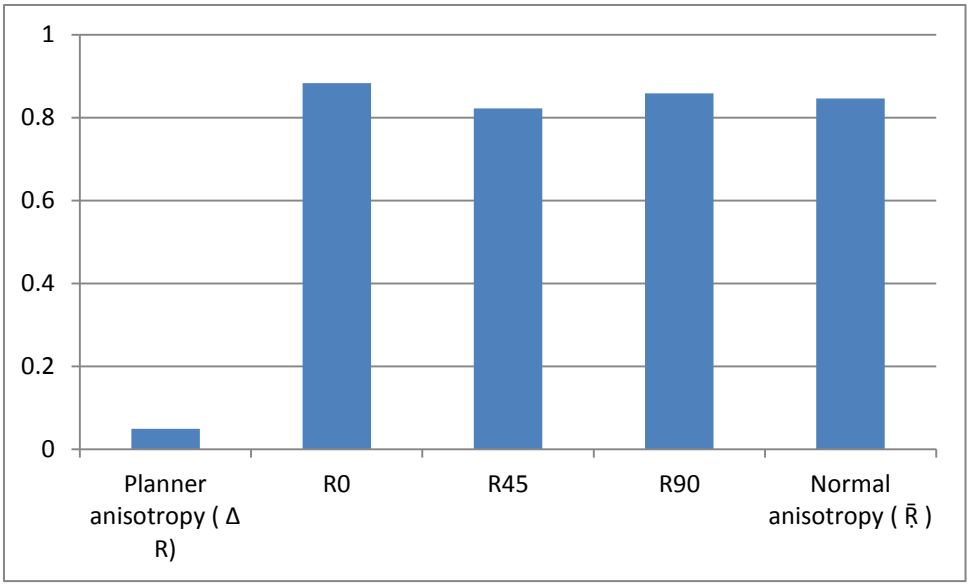

Figure 38: Comparative graphs of various anisotropic values of 16 SWG sheets

7.3 Effect of strain rate on anisotropic behaviour

The results of experimental studies are shown in Table 4. It is observed that as the plastic strain increases from 15% to a maximum of 35% during tension test, the average plastic strain ratio increases from 0.988 to 1.122 respectively and the same trend is seen in the values of planar anisotropy which varies between a minimum of 0.025 and maximum of 0.149. The equivalent plastic strain during deep drawing can be as high as 40%, therefore anisotropic behaviour at 35% of plastic strain is more accurate and significant to be used in simulations.

Table 4: Measured normal and planar anisotropy after uniaxial tension test

Plastic strain	Specimen orientation to rolling direction	Initial gage length (mm)	Final gage length (mm)	Initial average width (mm)	Final average width (mm)	Plastic strain ratio (R)	Normal anisotropy $\bar{R}$	Planar anisotropy ΔR
15%	0°	49.53	52.86	12.60	12.20	0.992	0.988	0.025
	45°	50.21	53.94	12.54	12.10	0.975		
	90°	50.11	53.46	12.50	12.10	1.010		
20%	0°	50.20	54.95	12.36	11.79	1.101	1.066	0.063
	45°	50.31	54.82	12.31	11.79	1.034		
	90°	50.32	54.72	12.32	11.79	1.094		
25%	0°	49.71	55.47	12.60	11.89	1.136	1.103	0.084
	45°	49.72	55.94	12.46	11.73	1.061		
	90°	49.81	55.91	12.55	11.80	1.155		
30%	0°	50.15	57.46	12.53	11.65	1.145	1.117	0.094
	45°	49.92	57.43	12.47	11.60	1.070		
	90°	49.92	56.96	12.60	11.73	1.183		
35%	0°	50.32	58.24	12.66	11.72	1.149	1.122	0.149
	45°	50.10	59.10	12.43	11.43	1.047		
	90°	50.31	59.10	12.53	11.43	1.246		

It is illustrated in the Figure 39 that in each tensile test, highest plastic strain is observed in specimen orientated at 90° to rolling direction followed by orientations of 0° and 45° respectively.

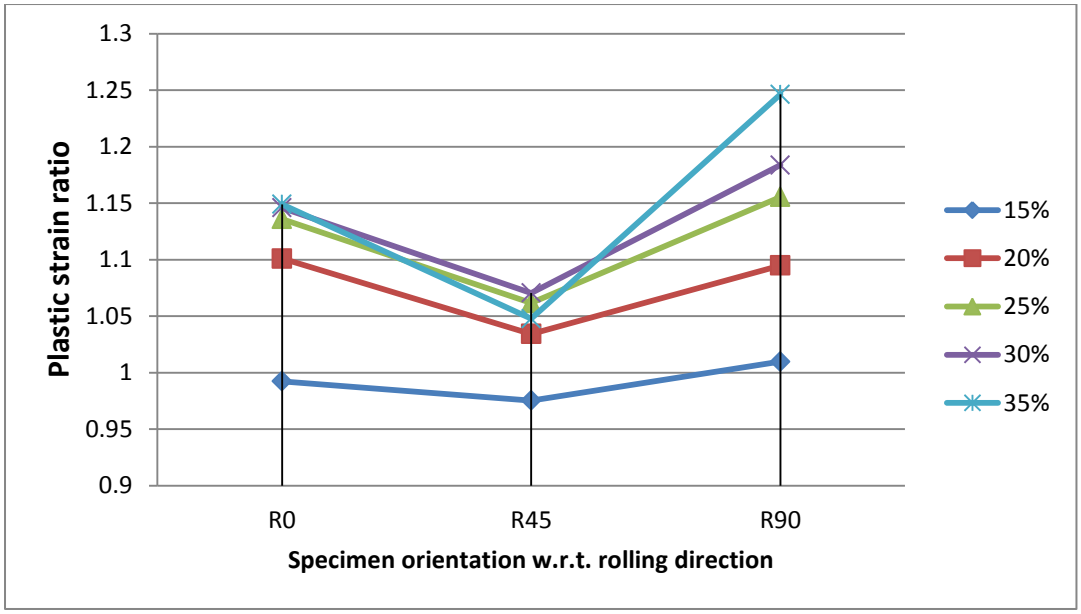

Figure 39: Variation of Plastic strain ratio with respect to rolling direction

7.6 Tensile properties of As Rolled (AR) specimens

7.4.1 Stress strain curve

Typical engineering stress-engineering strain curve and a true stress-true strain curve of AR specimens of thickness gauge 22 SWG corresponding to orientation 0, 45 and 90 degree to rolling direction are shown Figure 40. Similarly 20 SWG are shown in Figure 41 and 16 SWG are shown in Figure 42.

The value of yield strength i.e. onset of permanent deformation, was manually after careful analysis of engineering stress vs. strain curve. The values of strength (YS and UTS) and ductility (% elongation) show a large variation in mechanical properties. Ultimate Tensile Strength (UTS) was determined by maximum load and original cross-section area of the specimen.

It can be seen that the average yield stress of 22 SWG specimens were in the range of 931 – 1146 MPa and average UTS were in the range of 1328 – 1411 MPa. For 20 SWG specimens average yield stress were in the range of 1374 – 1408 MPa and UTS were in the range of 1418 – 1481 MPa. For 16 SWG average yield stress were in the range of 793 – 864 MPa and average UTS were in the range of 1109 – 1171 MPa.

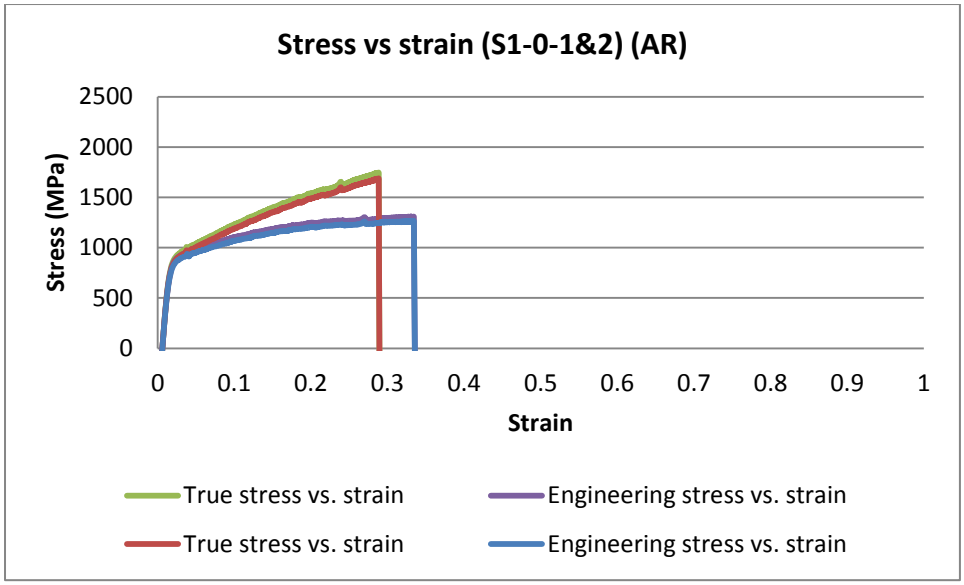

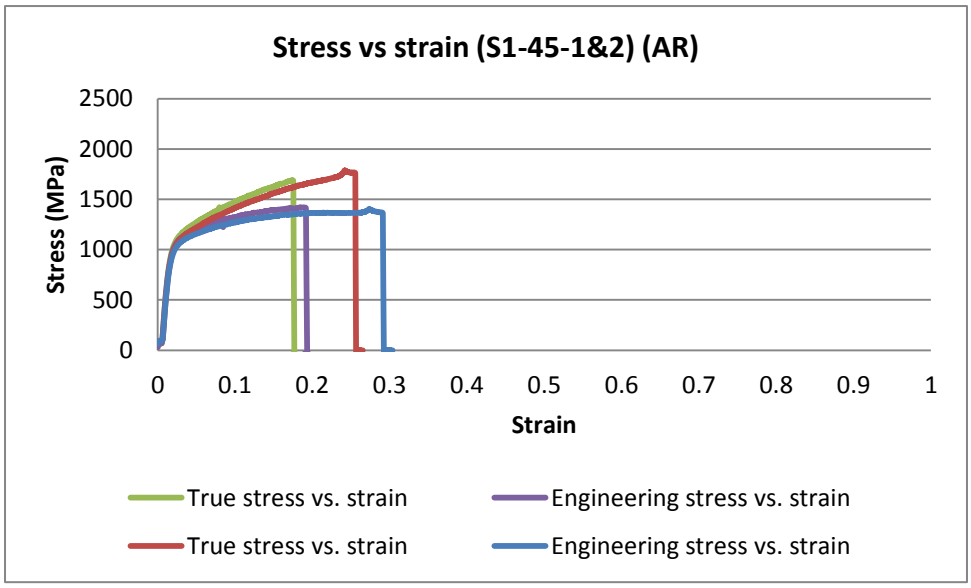

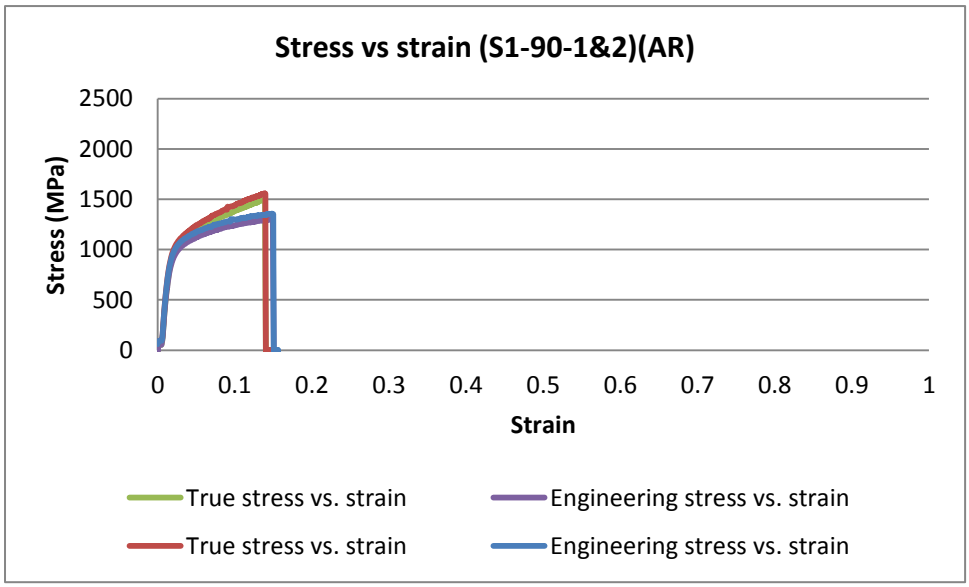

Figure 40: E. Stress vs. strain and True stress vs. strain curve of 22 SWG (0.6 mm) thickness specimen

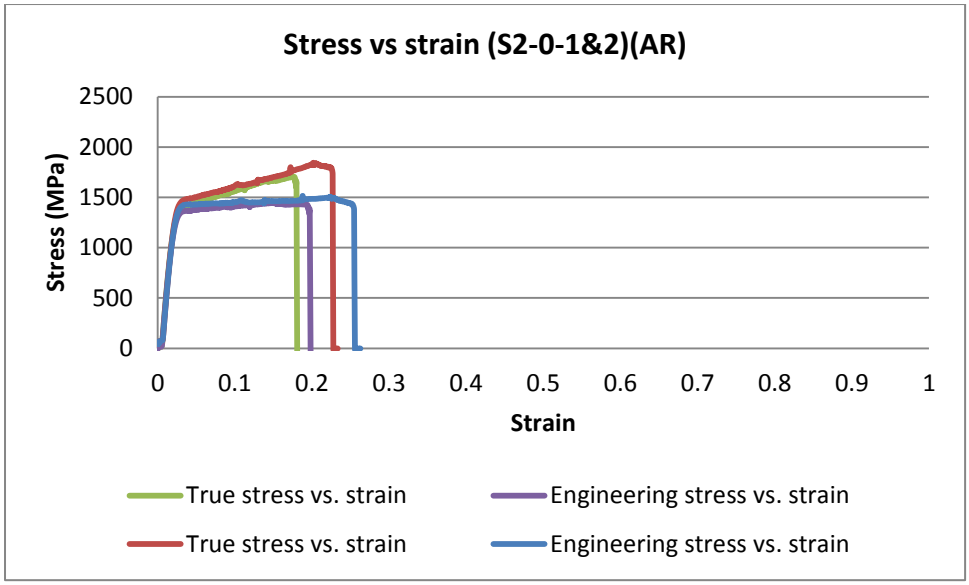

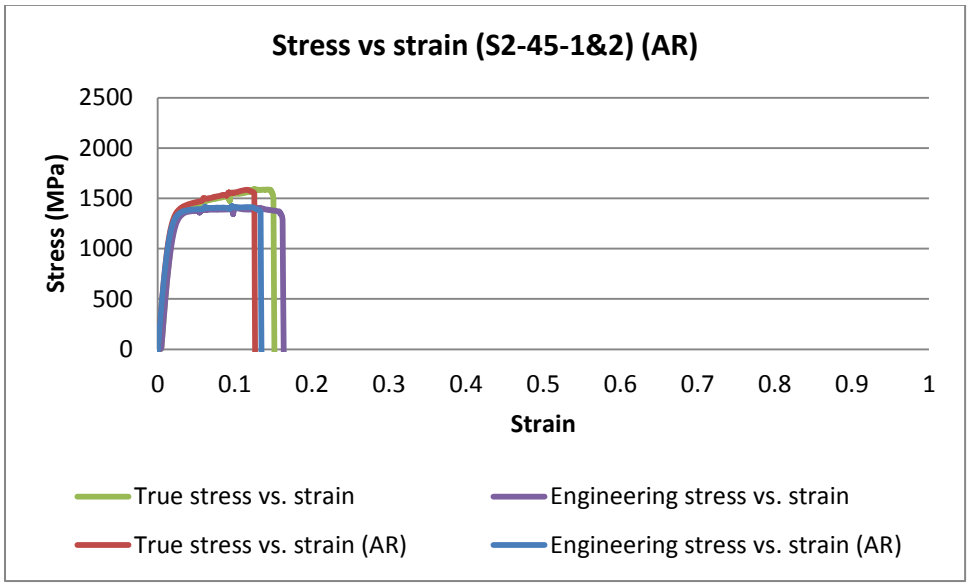

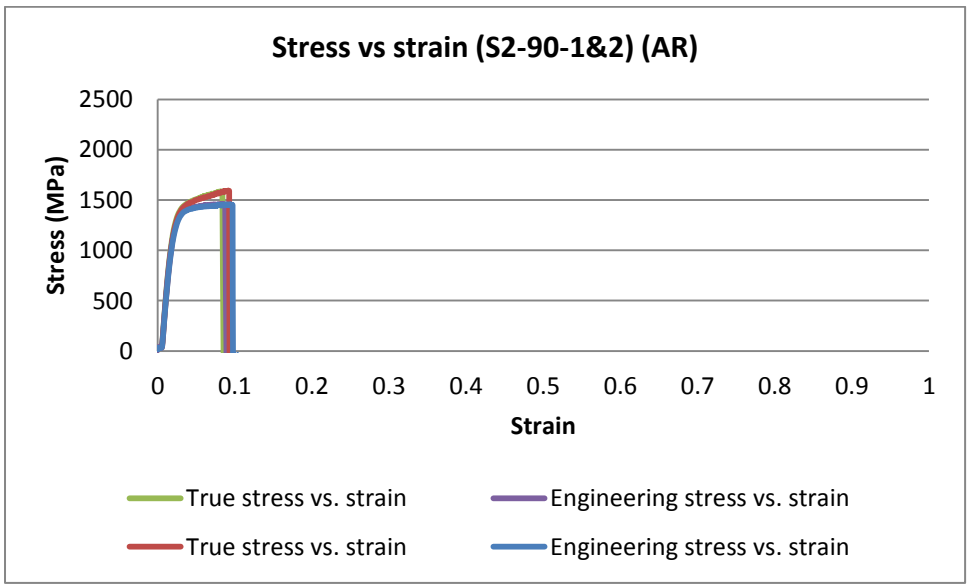

Figure 41: E. Stress vs. strain and True stress vs. strain curve of 20 SWG (0.8 mm) thickness specimens

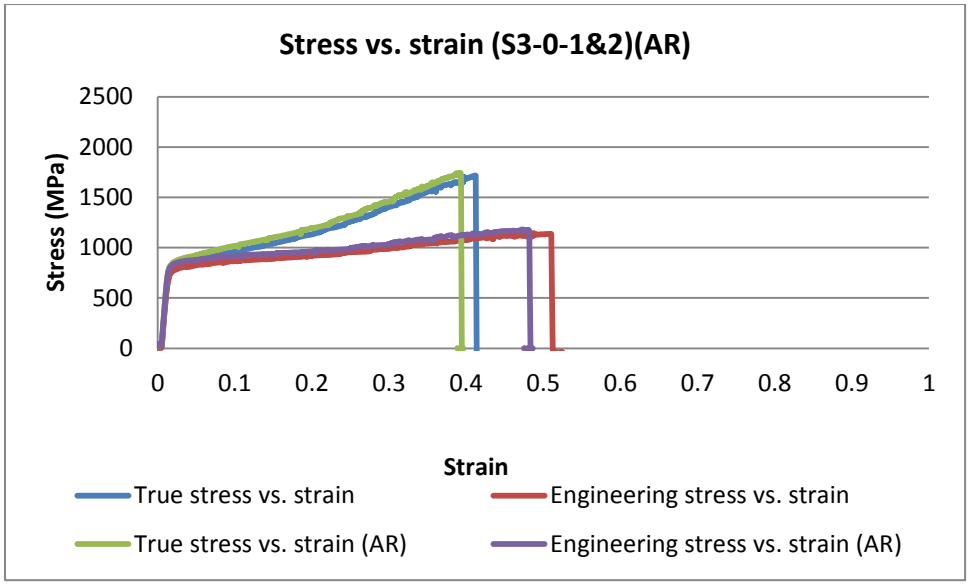

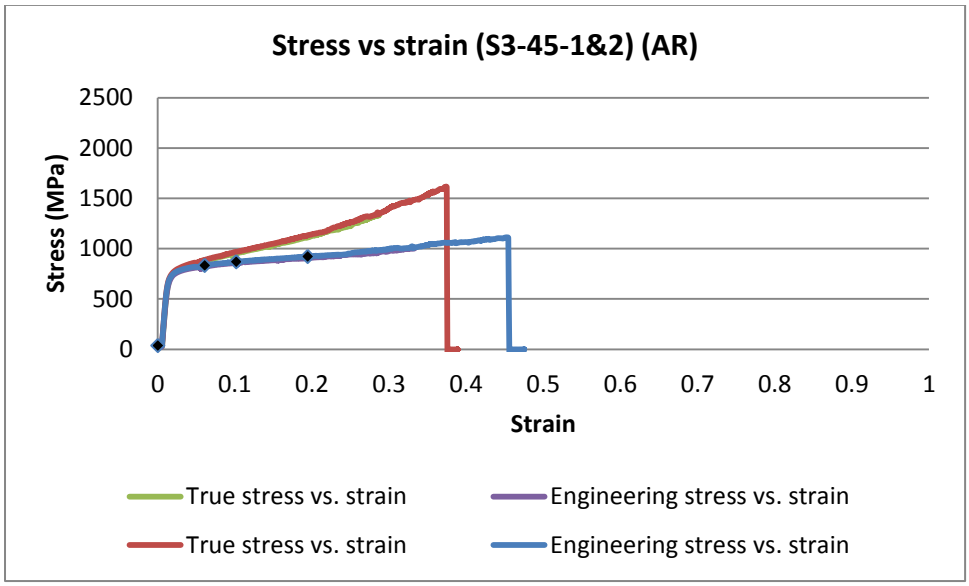

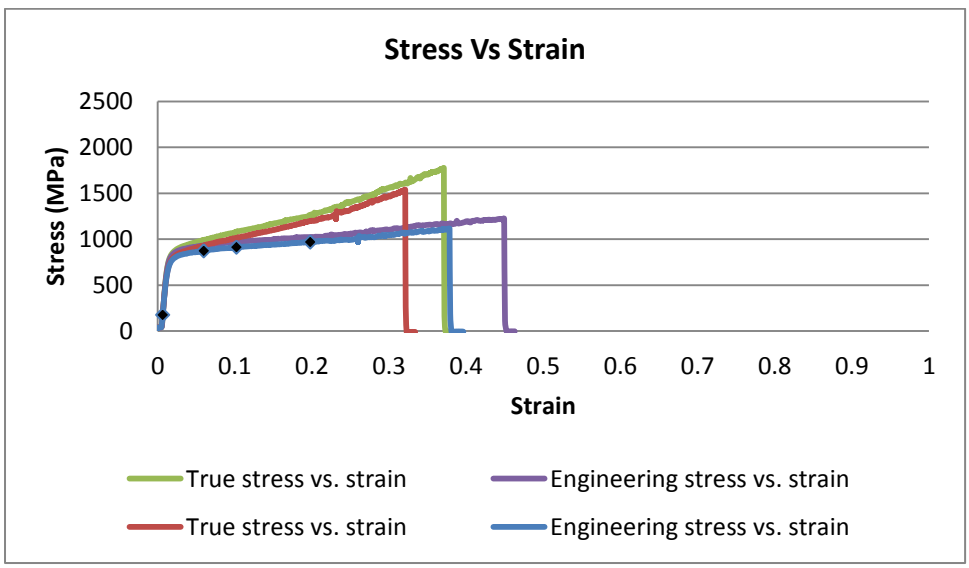

Figure 42: E. Stress vs. strain and True stress vs. strain curve of 16 SWG (1.4 mm) thickness specimens

7.5 Anisotropic properties of AR specimens

7.5.1 Thickness 22 SWG (~0.67 mm) specimen

The planner anisotropy of 22 SWG specimen was found to be -0.15153 and normal anisotropy was found to be 0.930722. The details of the anisotropy of specimen in the direction parallel, diagonal and perpendicular are depicted in the Figure 43.

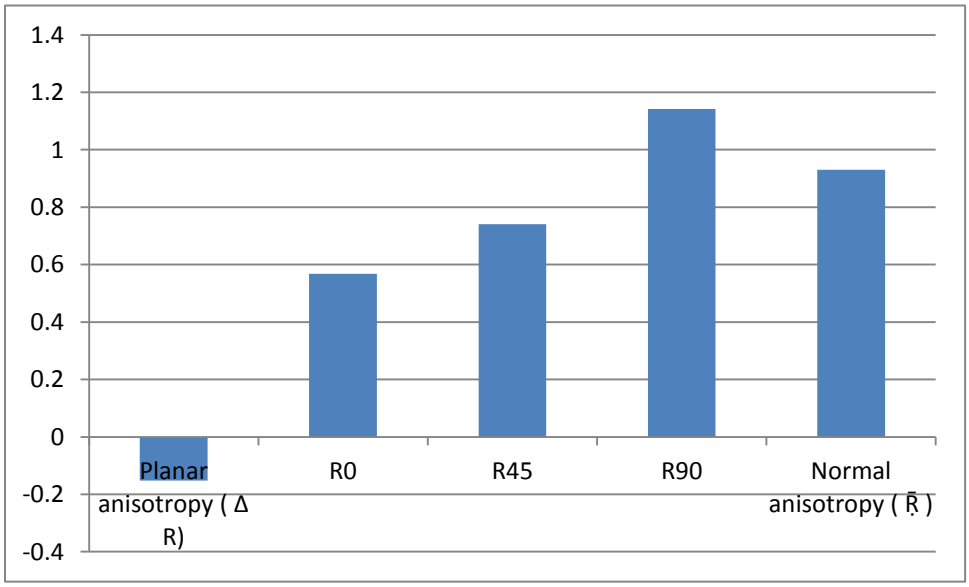

Figure 43: Comparative graphs of various anisotropic values of 22 SWG sheets

7.5.2 Thickness 20 SWG (~0.84 mm) specimen

The planner anisotropy of 20 SWG specimen was found to be 0.802216 and normal anisotropy was found to be 0.611428. The details of the anisotropy of sheet in the direction parallel, diagonal and perpendicular are depicted in the Figure 44.

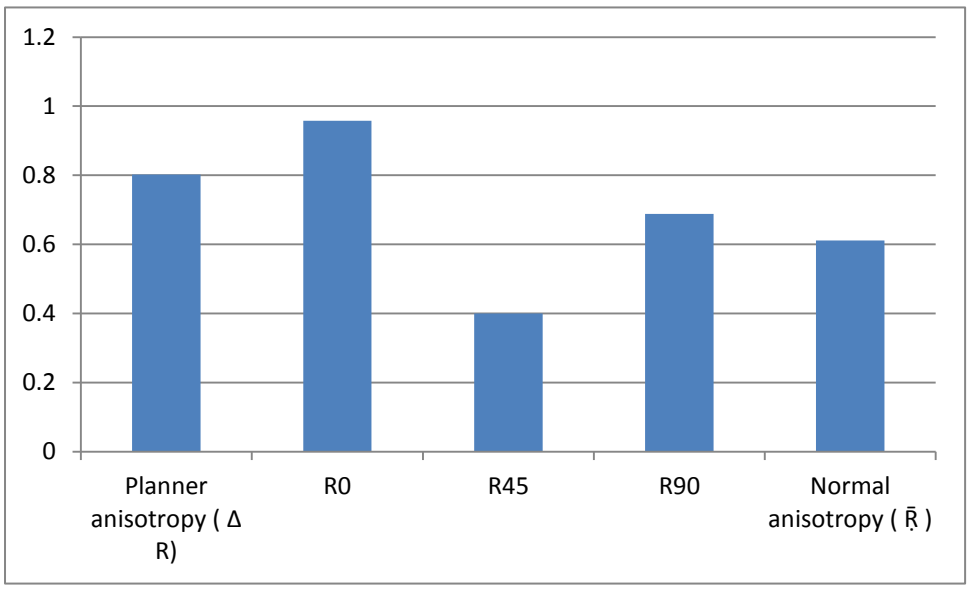

Figure 44: Comparative graphs of various anisotropic values of 20 SWG sheets

7.5.3 Thickness 16 SWG (~1.4 mm) specimen

The planner anisotropy of 16 SWG specimen was found to be 0.064237 and normal anisotropy was found to be 0.57575. The details of the anisotropy of sheet in the direction parallel, diagonal and perpendicular are depicted in the Figure 45.

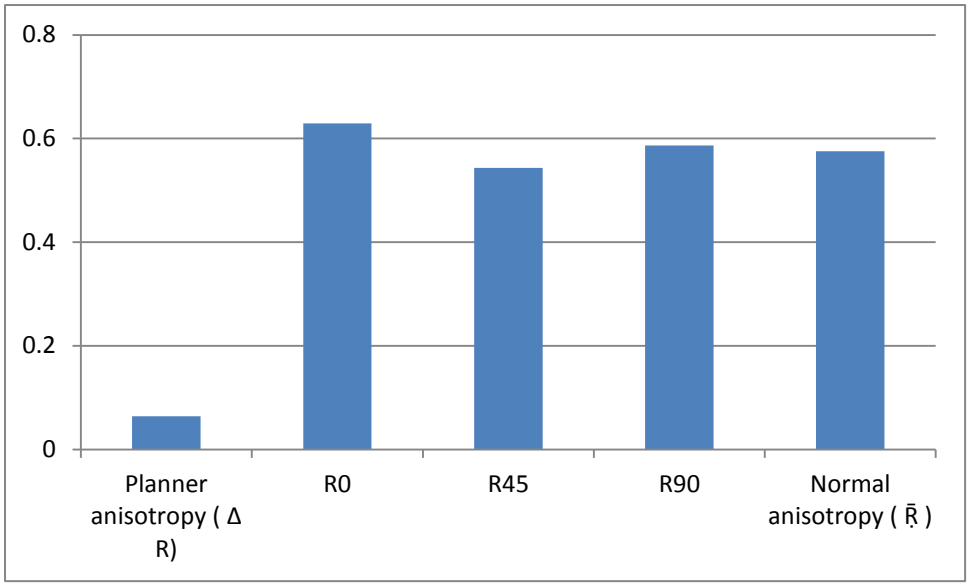

Figure 45: Comparative graphs of various anisotropic values of 16 SWG sheets

7.6 Comparison of tensile properties of AP & AR specimens

7.6.1 Stress strain curve

Typical comparative engineering stress-engineering strain curve and a comparative true stress-true strain curve of AR and AP specimens of all the three gauges are depicted in the Figures 46-54.

It can be seen that the average yield stress of AR specimens are almost 3.5 times of average yield stress of AP specimens. Average ultimate yield stresses of AR specimens are almost 1.4 times of average ultimate yield stress of AP specimens.

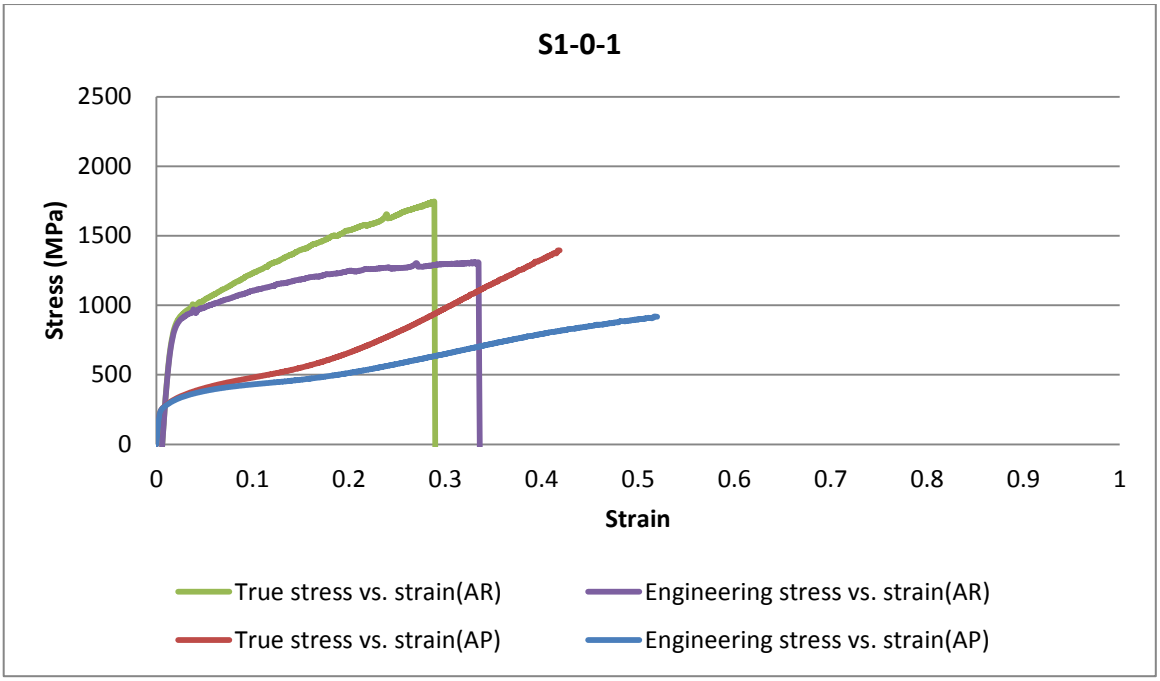

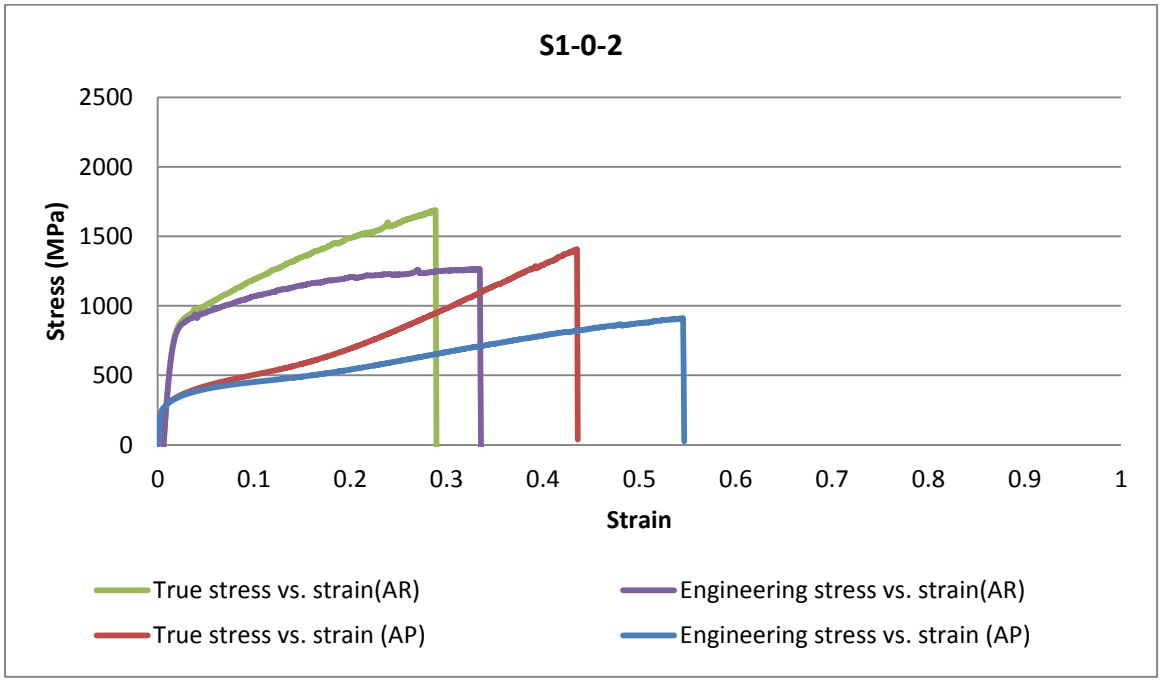

Figure 46: Comparison of stress vs. strain of AR & AP specimen- S1-0-1& 2

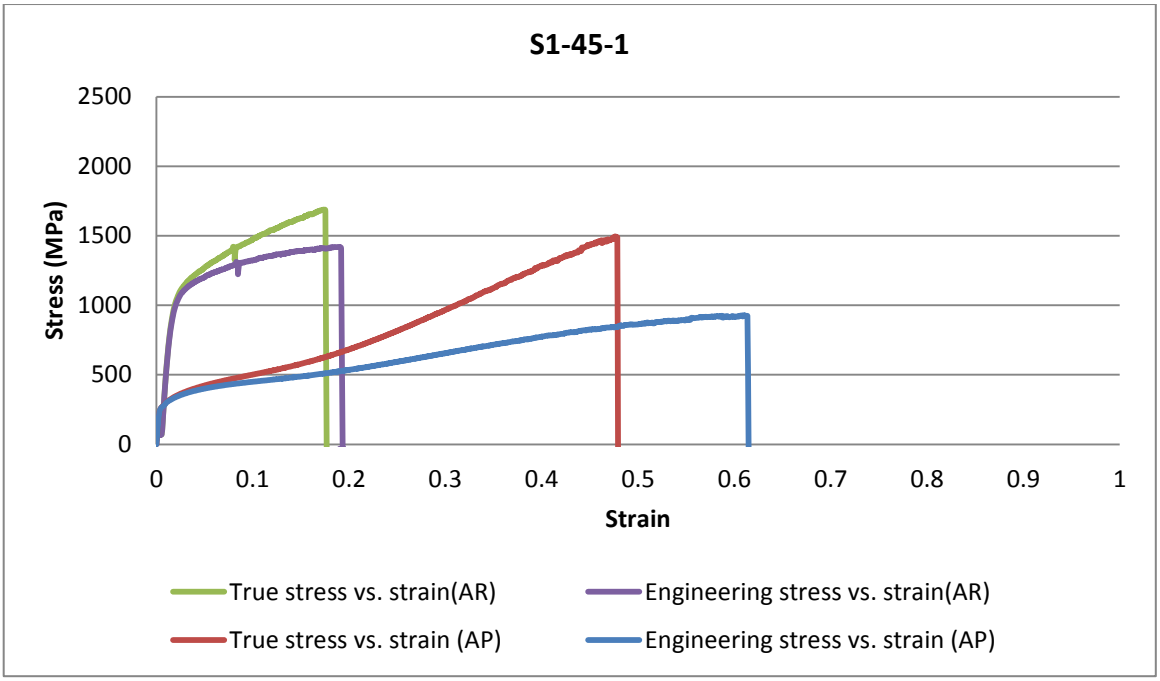

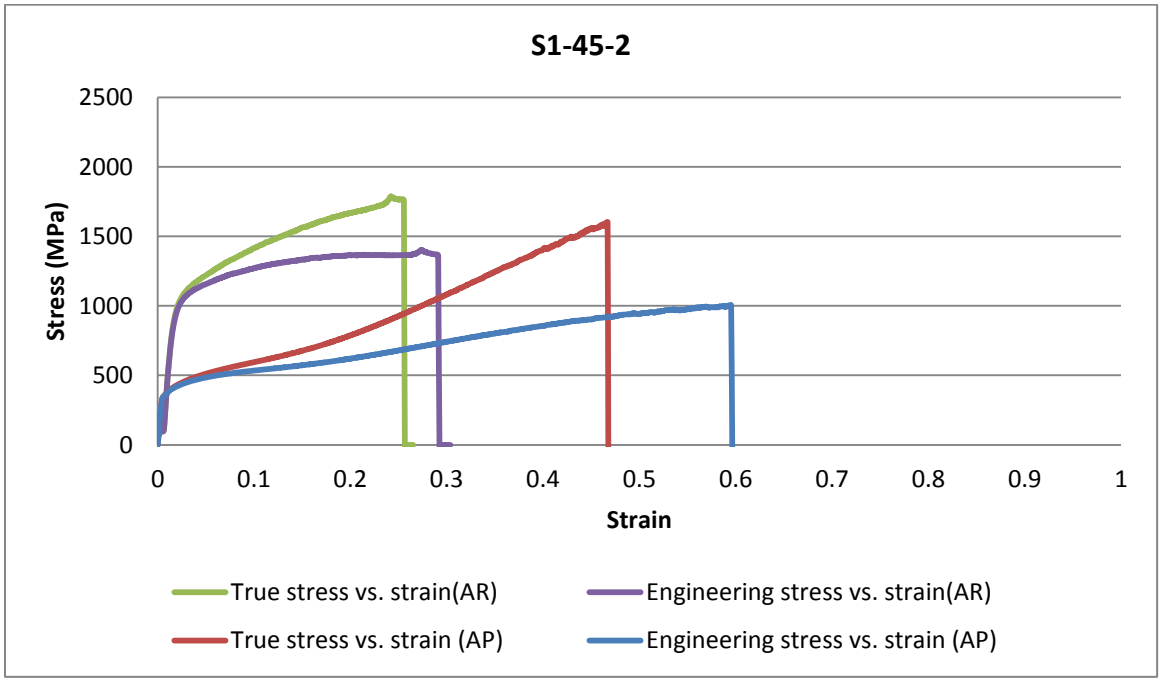

Figure 47: Comparison of stress vs. strain of AR & AP specimen- S1-45-1& 2

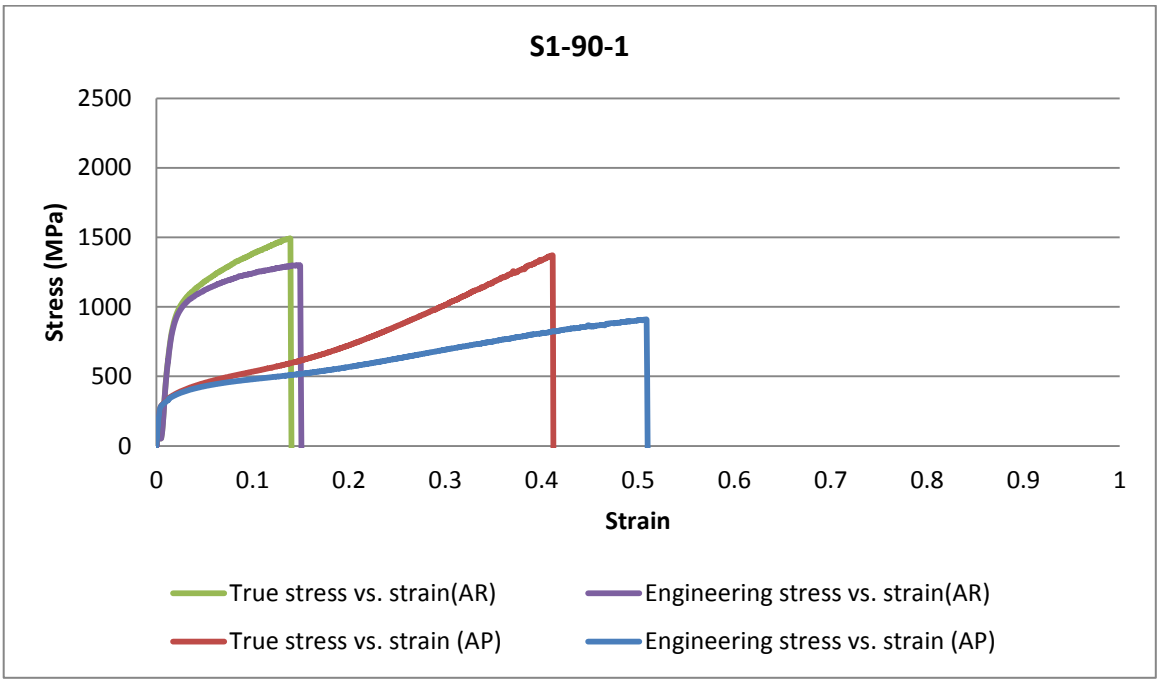

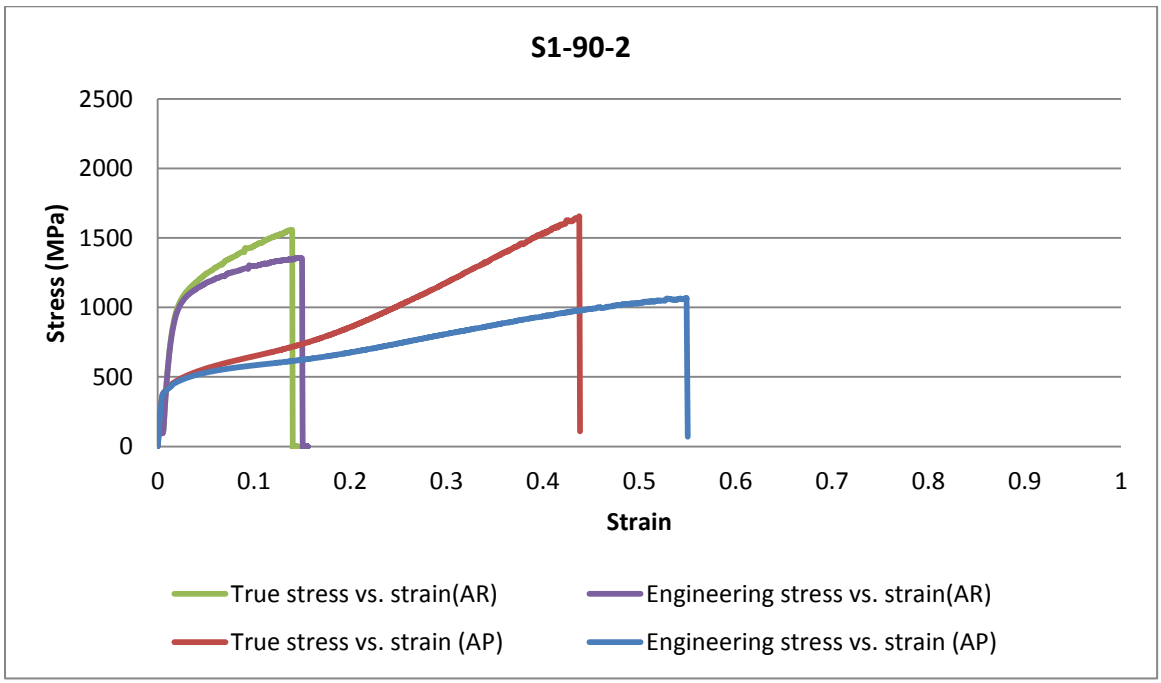

Figure 48: Comparison of stress vs. strain of AR & AP specimen- S1-90-1& 2

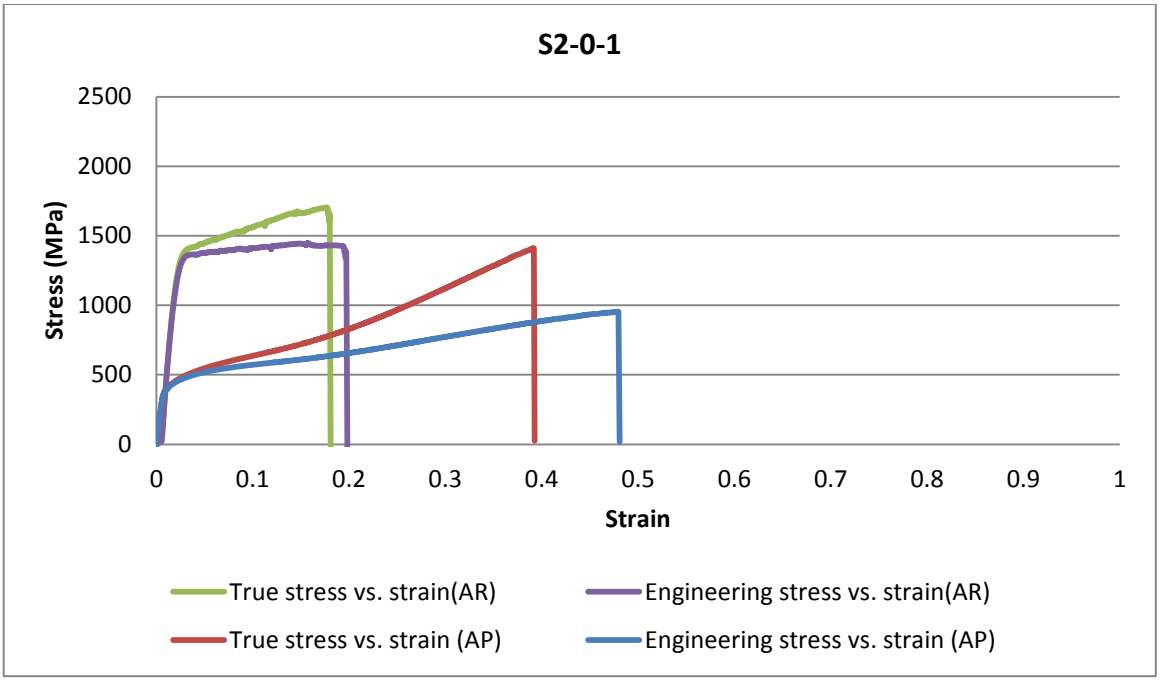

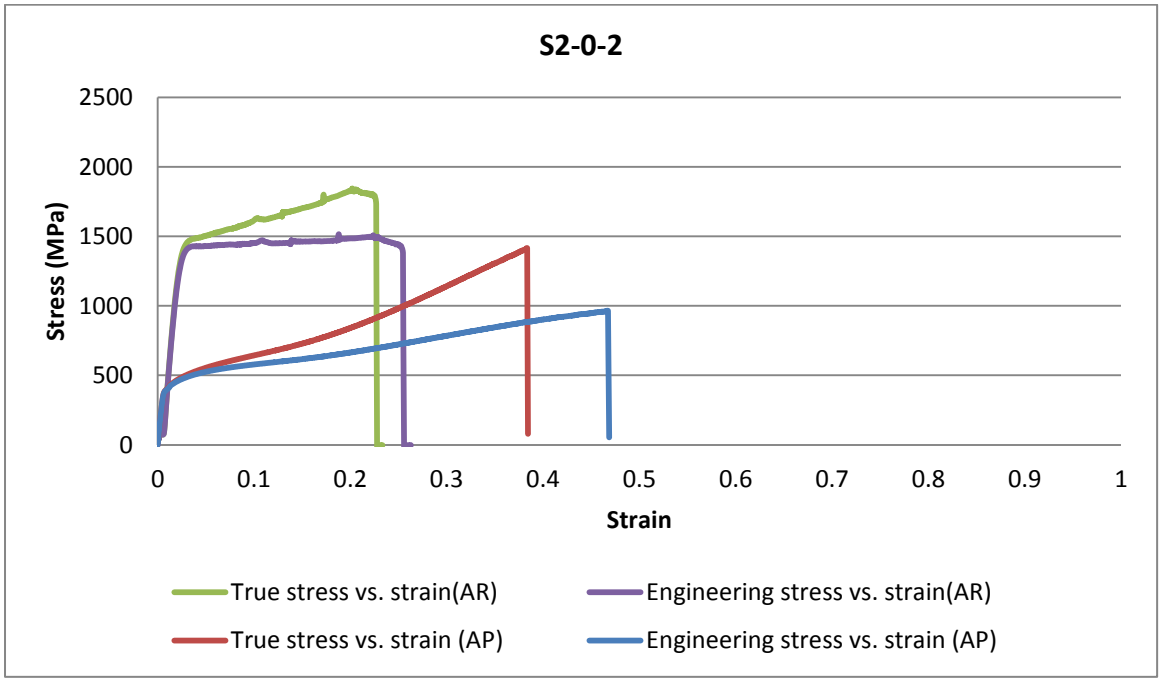

Figure 49: Comparison of stress vs. strain of AR & AP specimen- S2-0-1& 2

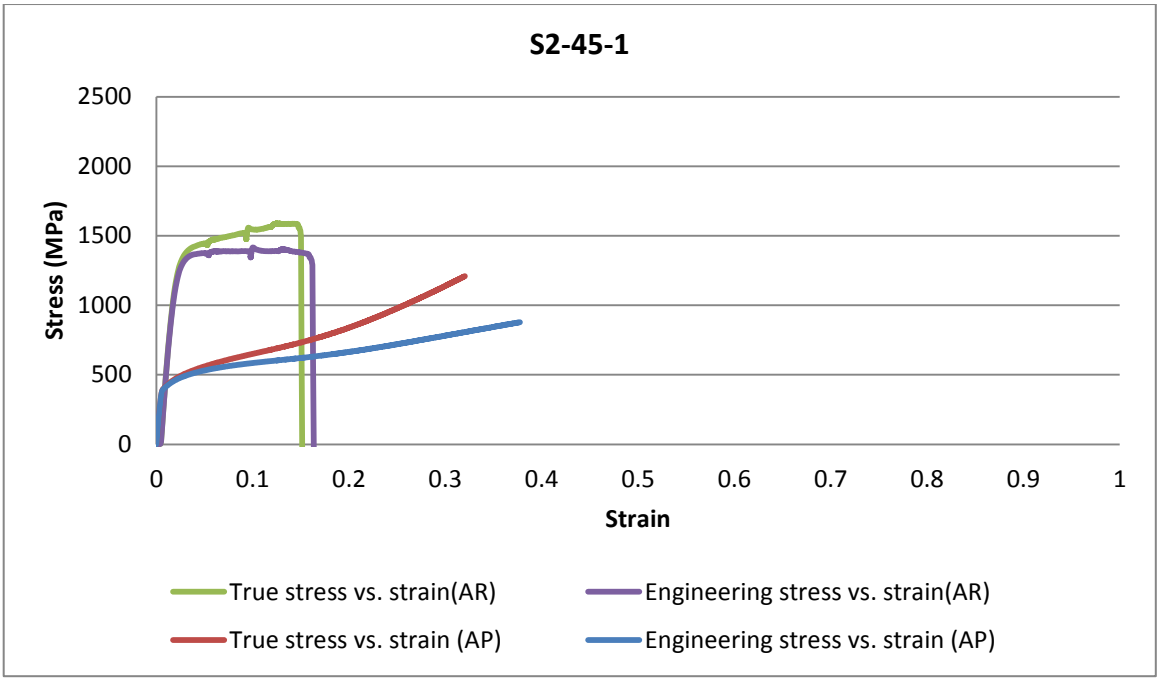

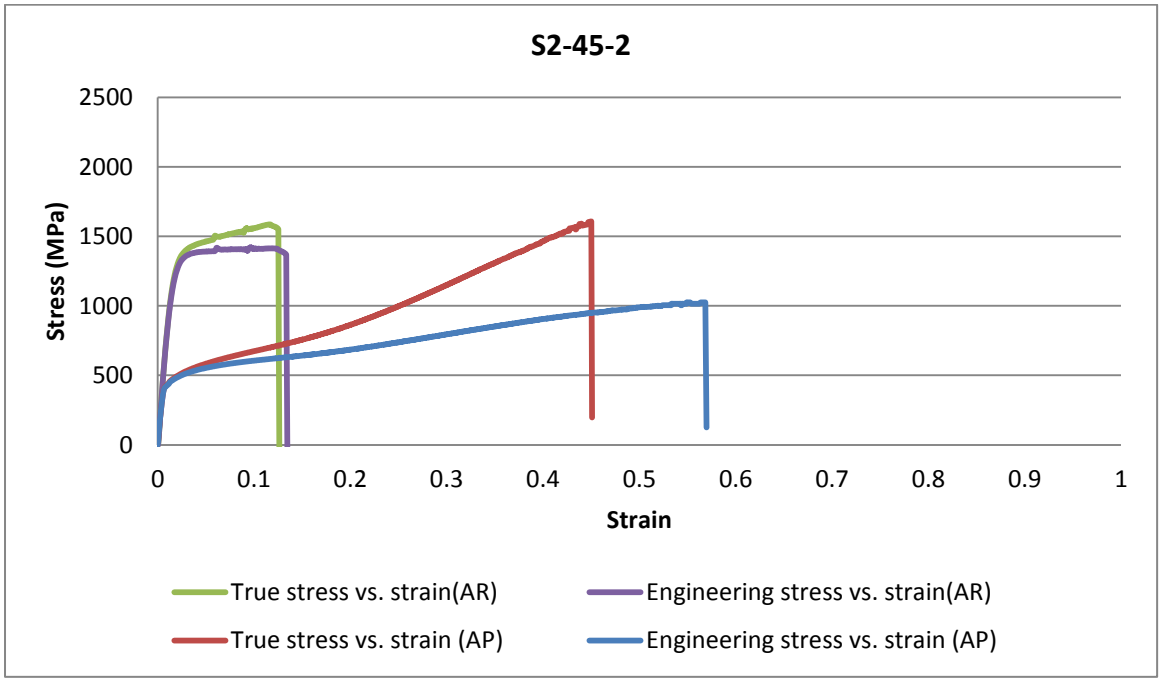

Figure 50: Comparison of stress vs. strain of AR & AP specimen- S2-45-1& 2

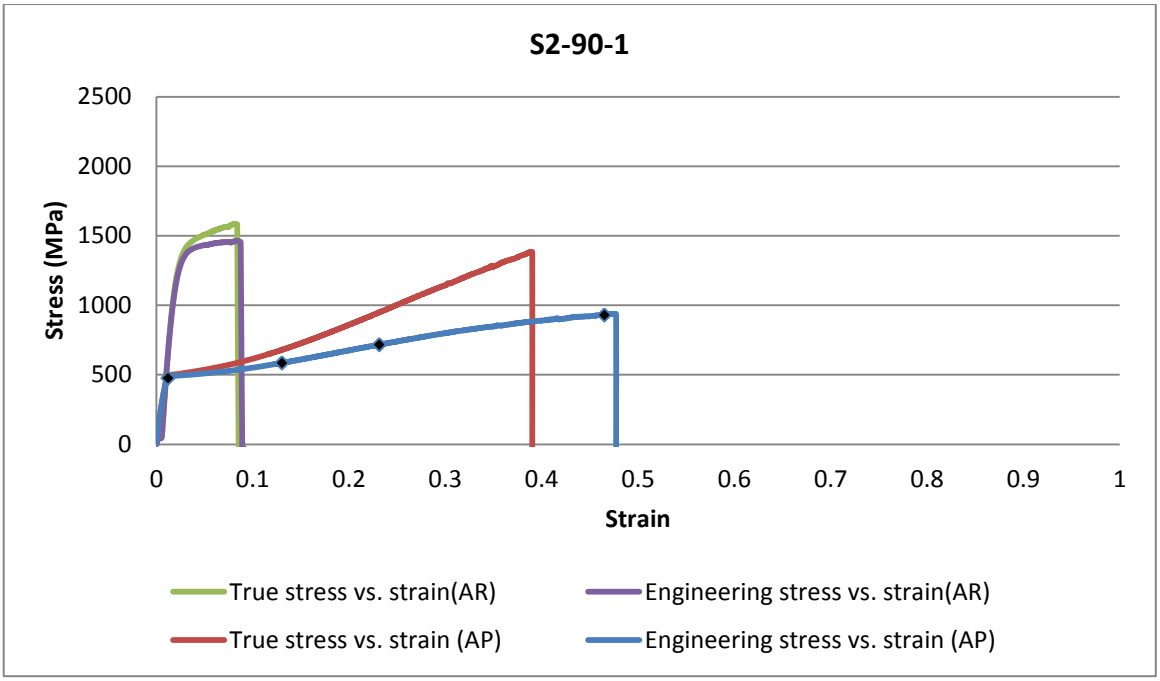

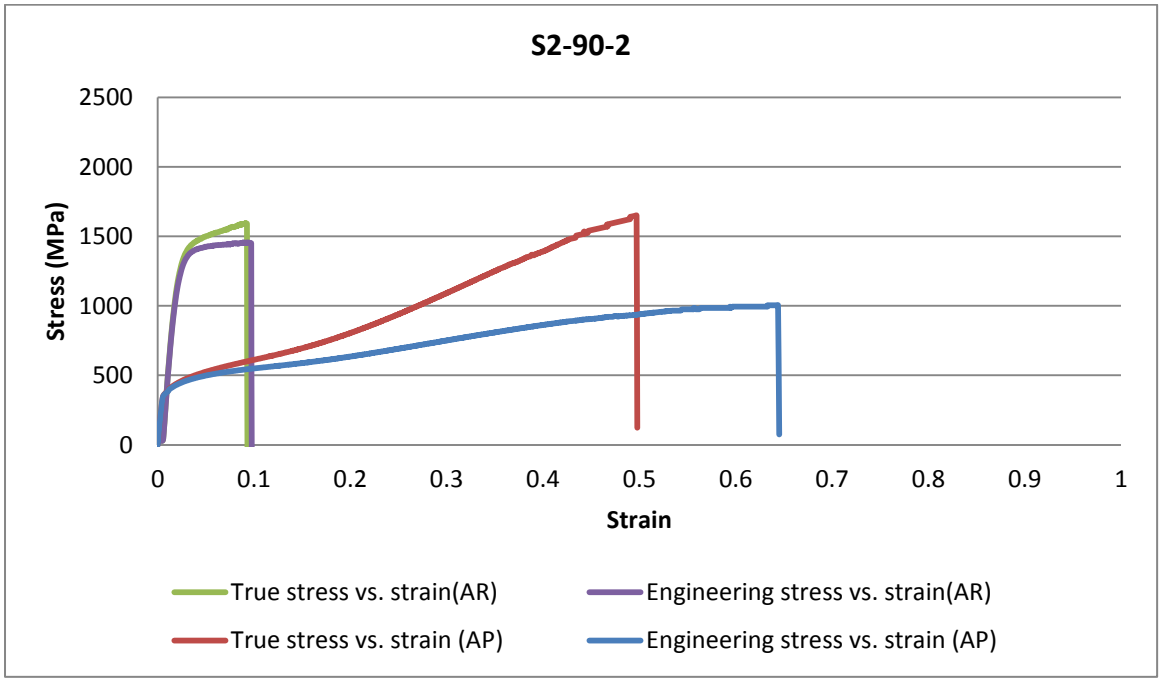

Figure 51: Comparison of stress vs. strain of AR & AP specimen- S2-90-1& 2

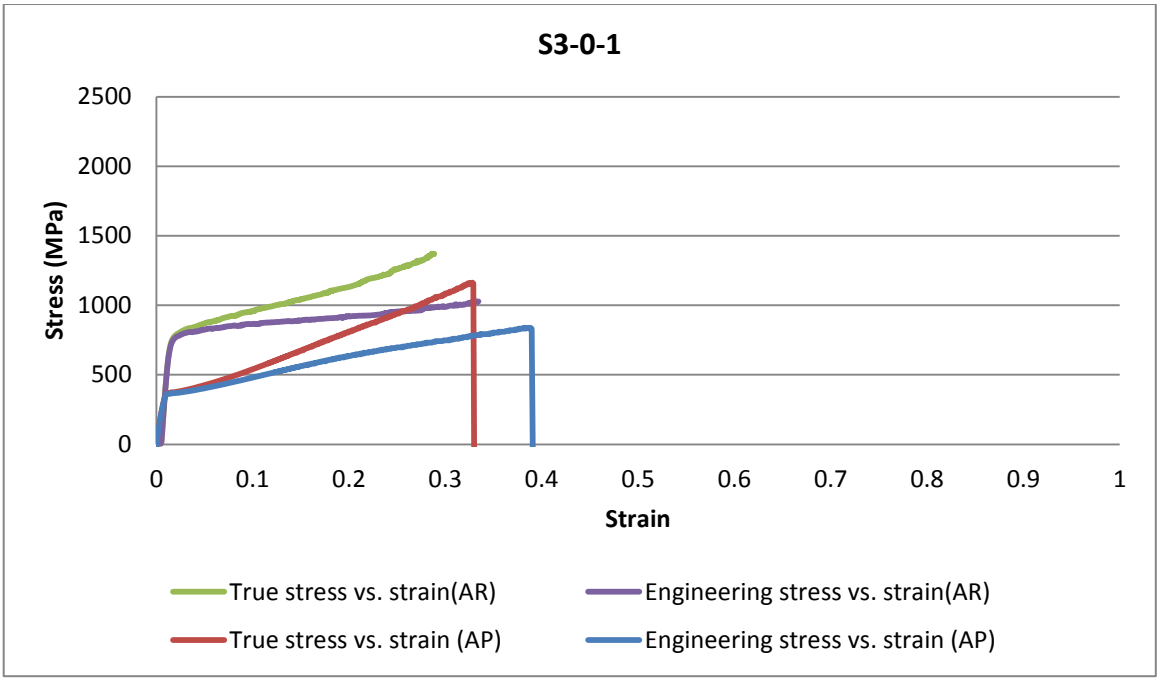

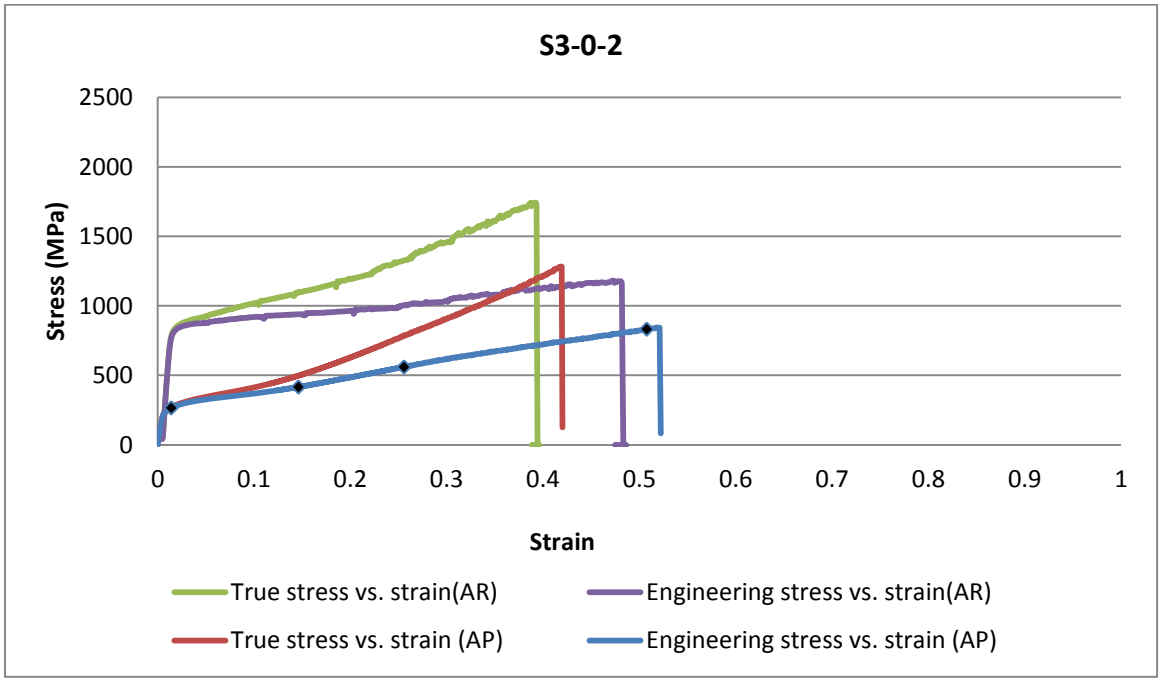

Figure 52: Comparison of stress vs. strain of AR & AP specimen- S3-0-1& 2

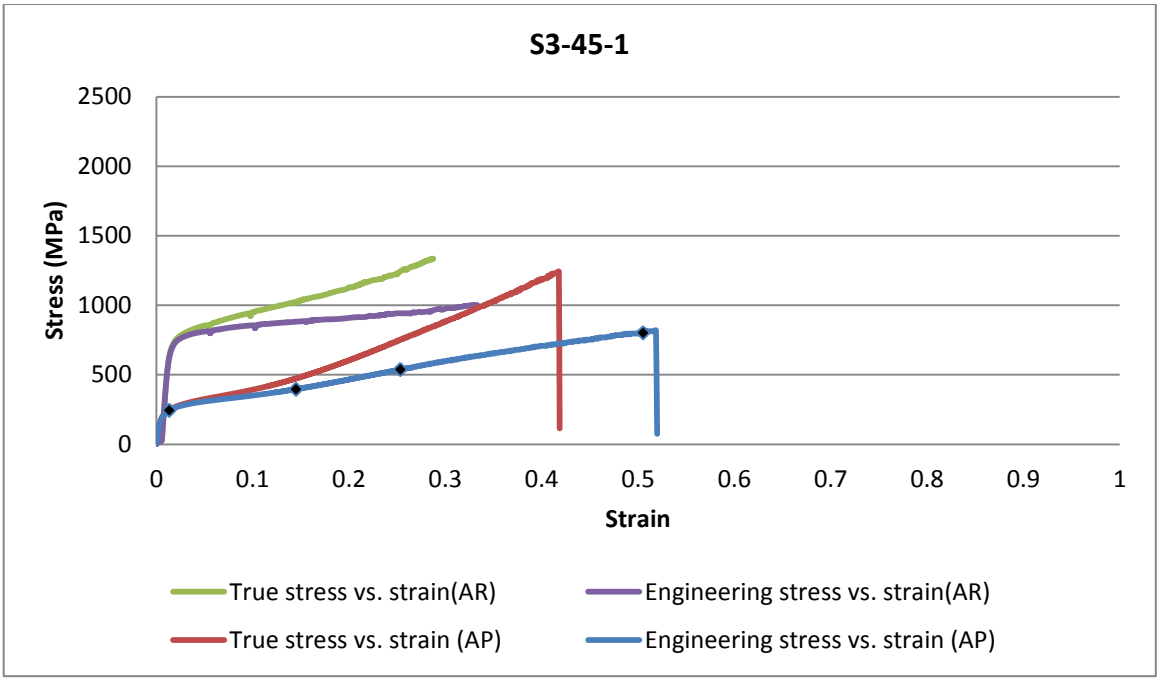

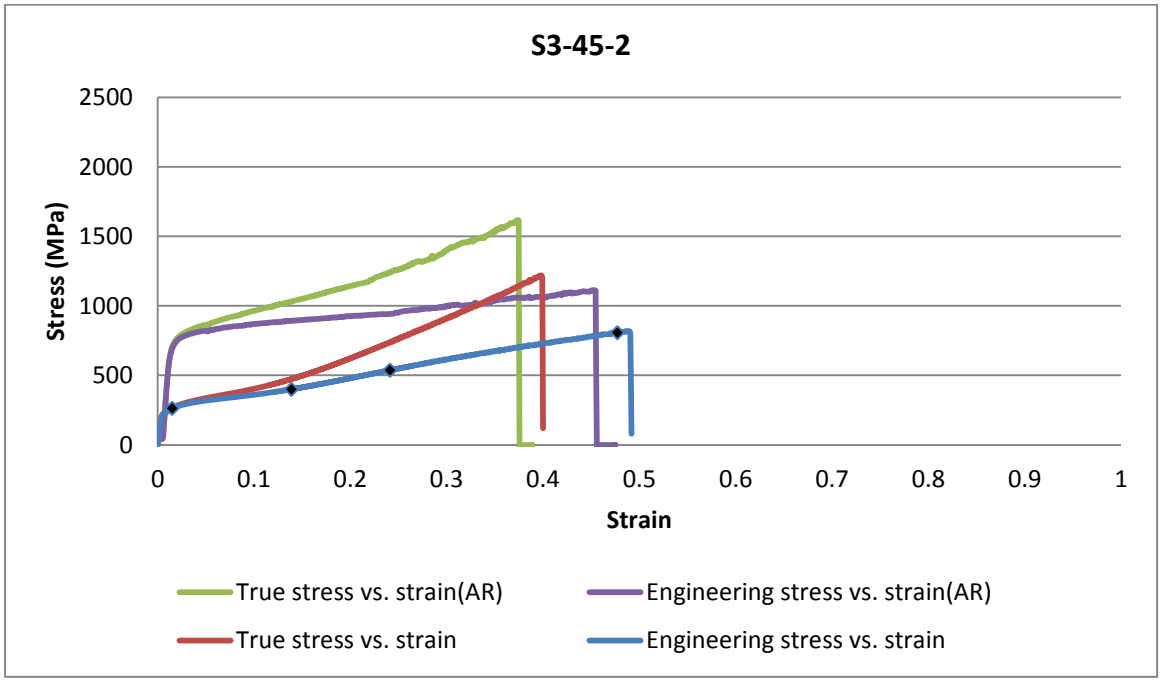

Figure 53: Comparison of stress vs. strain of AR & AP specimen- S3-45-1& 2

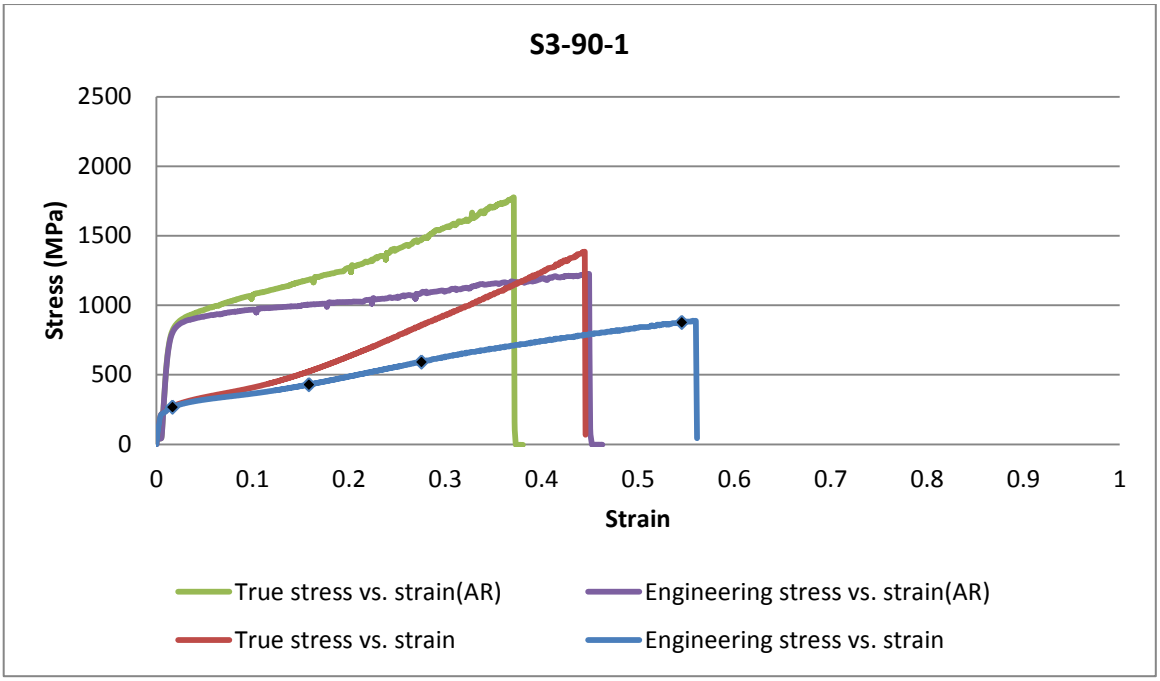

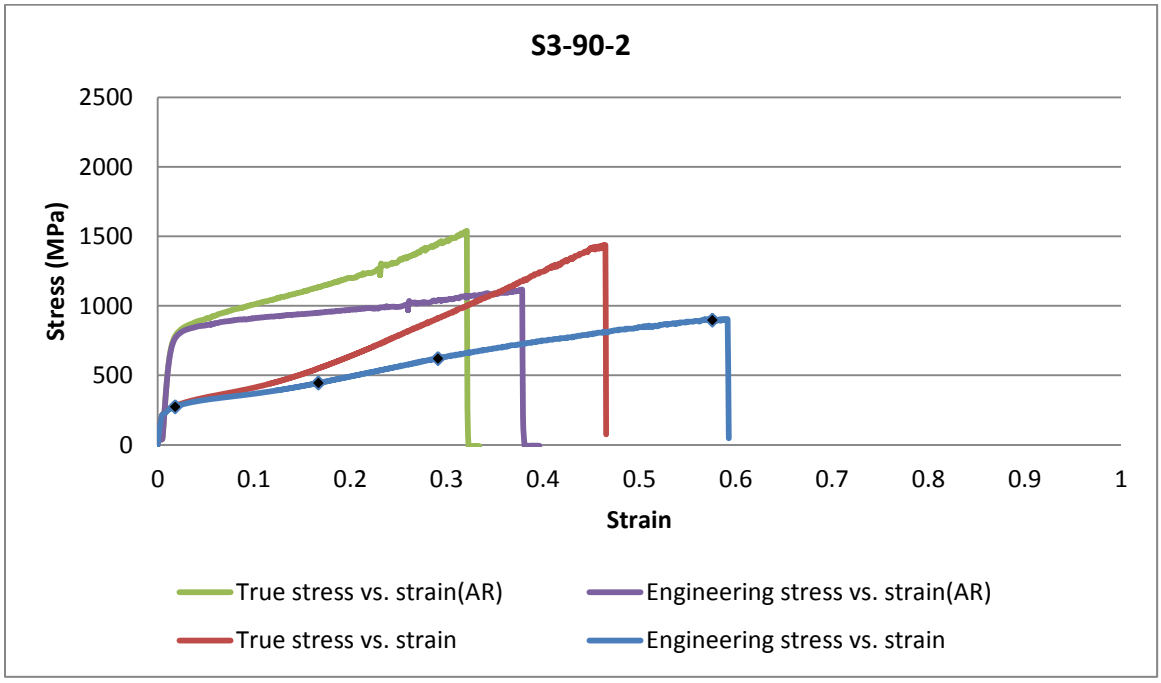

Figure 54: Comparison of stress vs. strain of AR & AP specimen- S3-90-1& 2

7.7 Microstructure observation

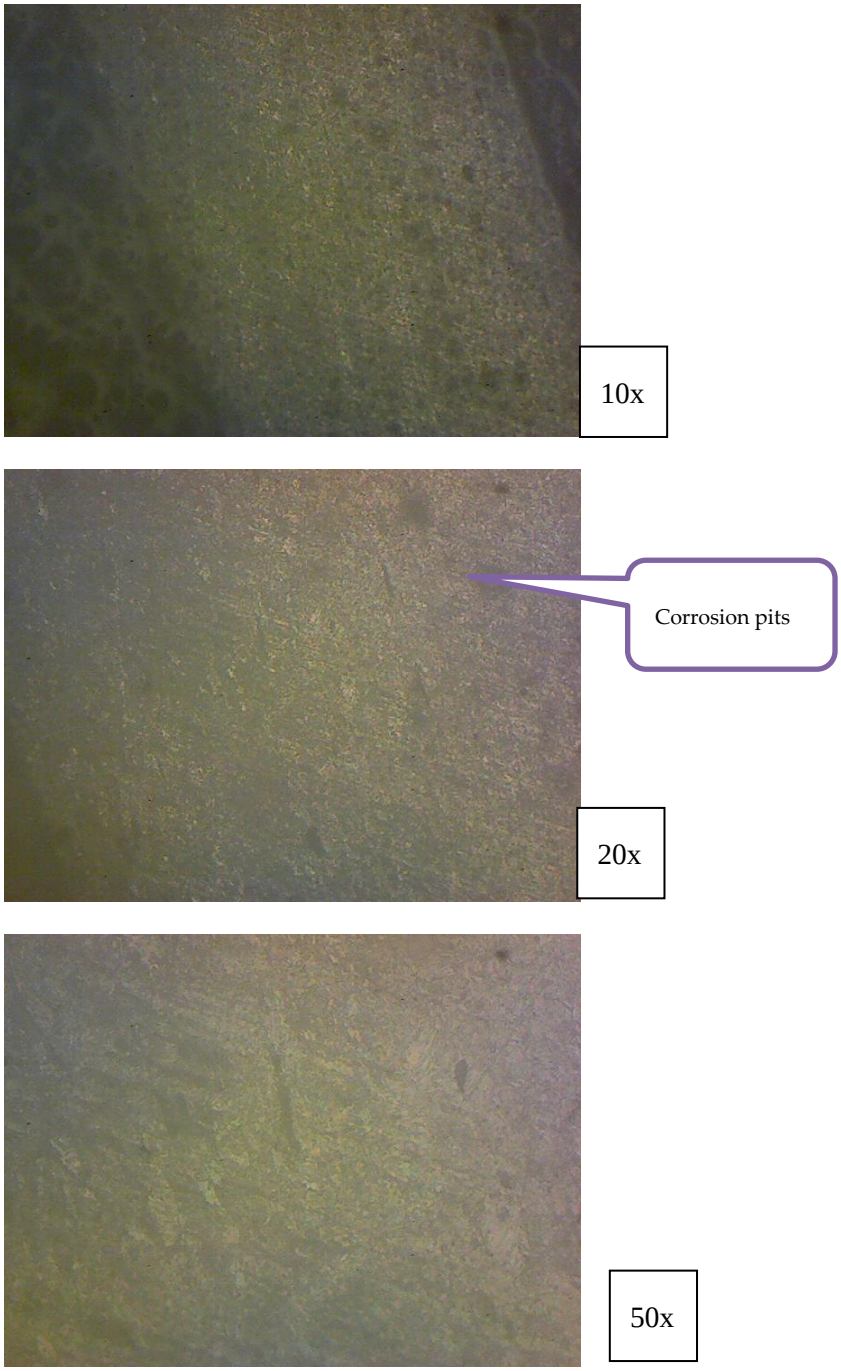

Figure 55: Observed microstructure of AR samples of 22 SWG (0.6 mm)

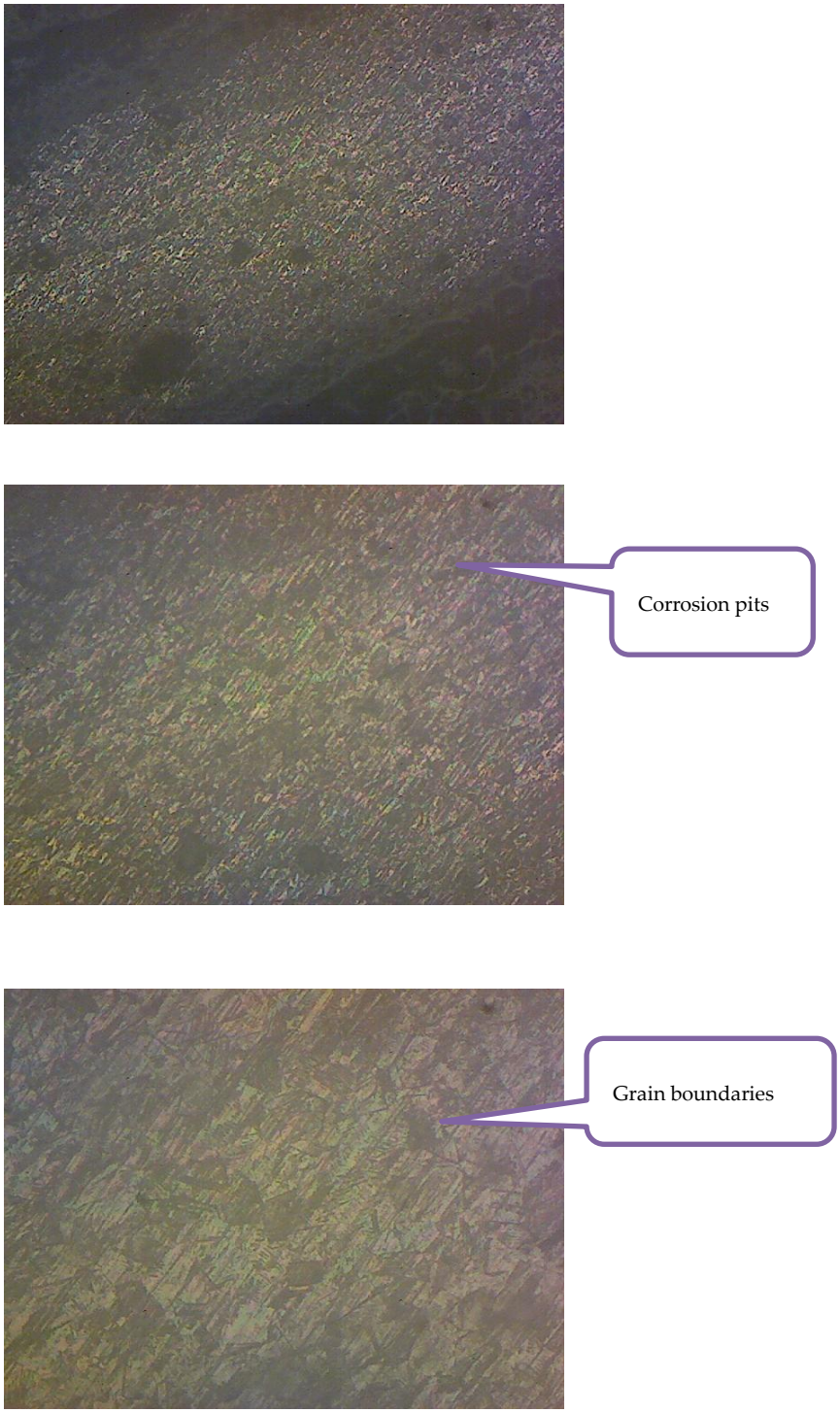

Figure 56: Observed microstructure of AP samples of 22 SWG (0.6 mm)

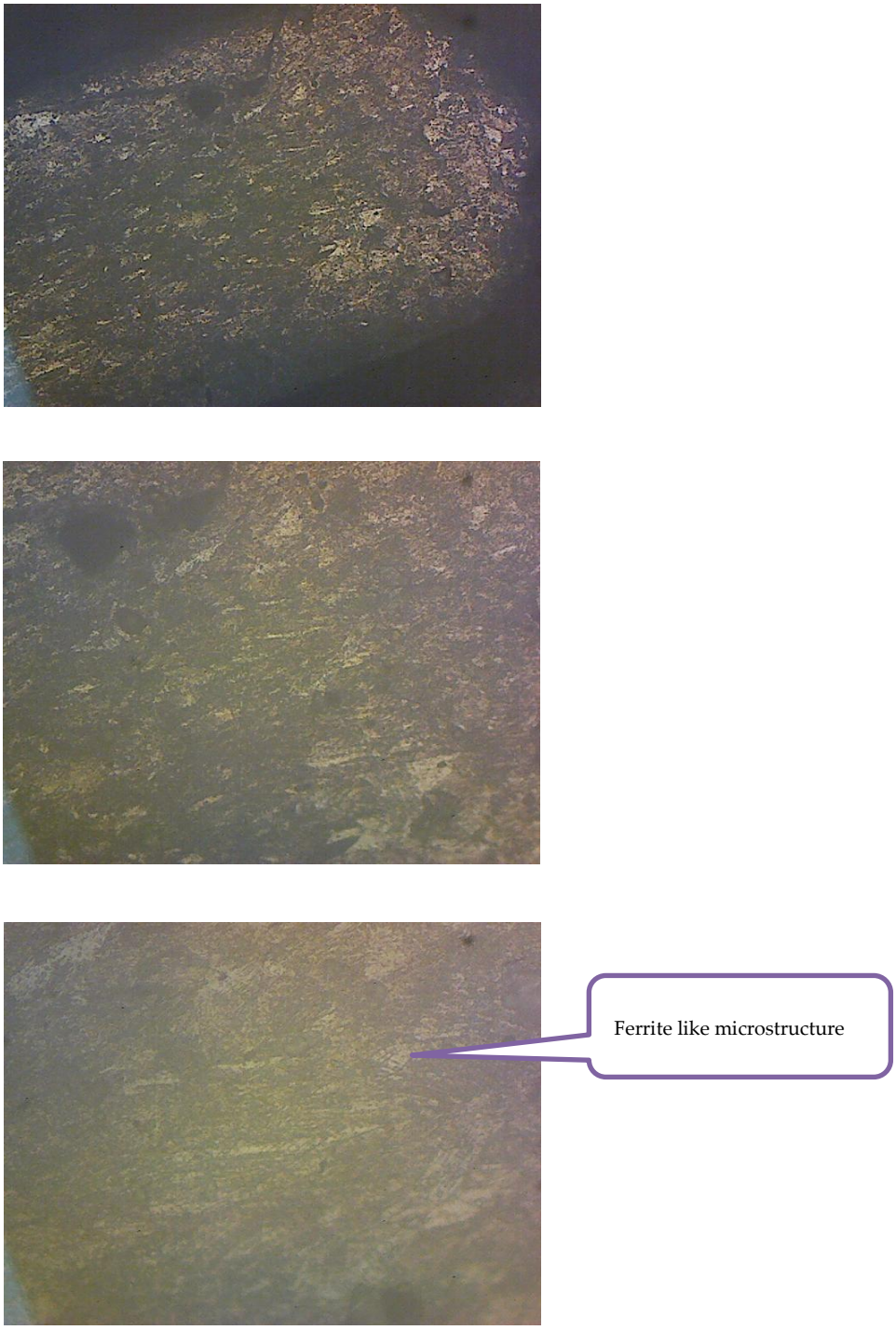

Figure 57: Observed microstructure of AR samples of 20 SWG (0.8 mm)

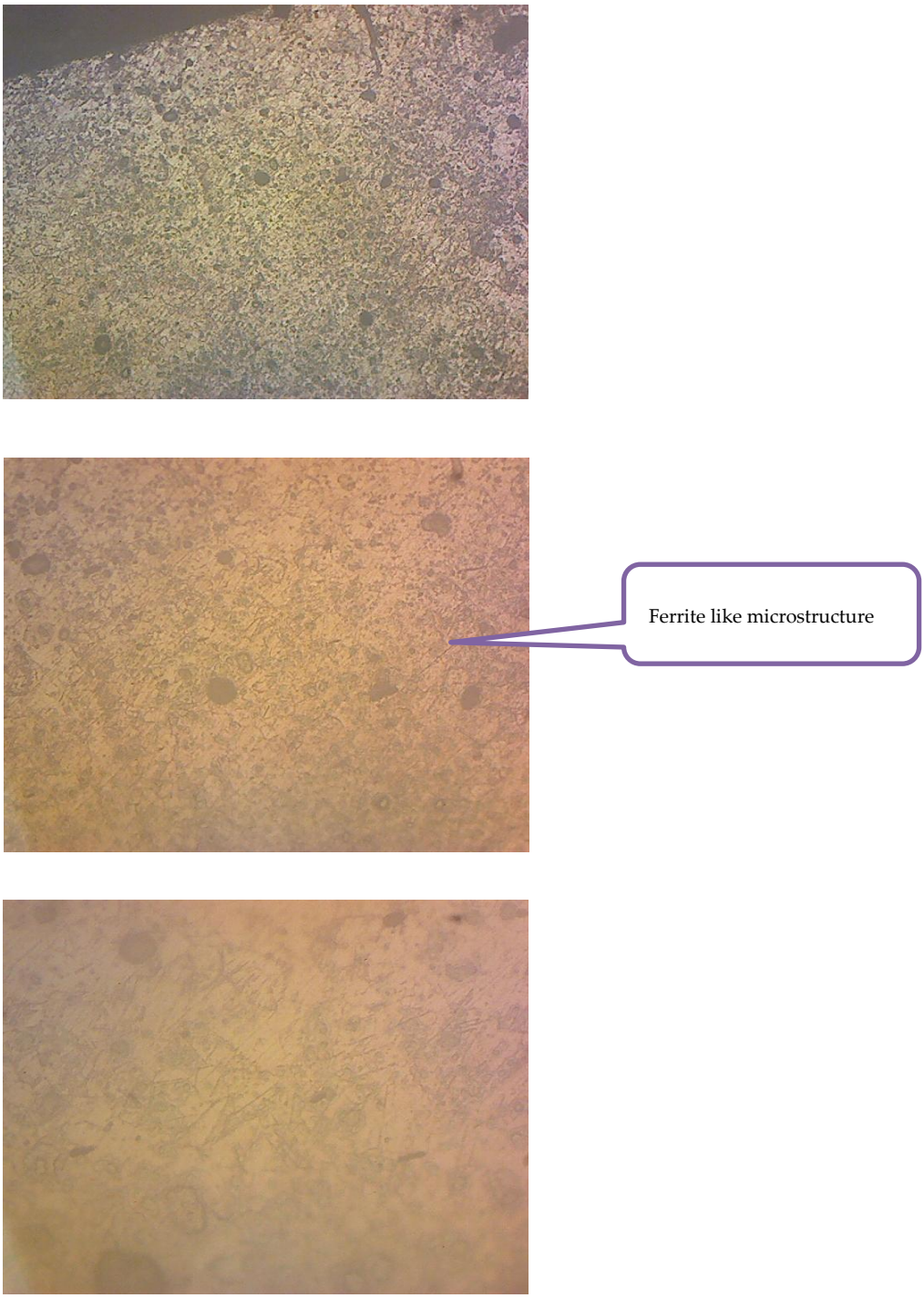

Figure 58: Observed microstructure of AP samples of 20 SWG (0.8 mm)

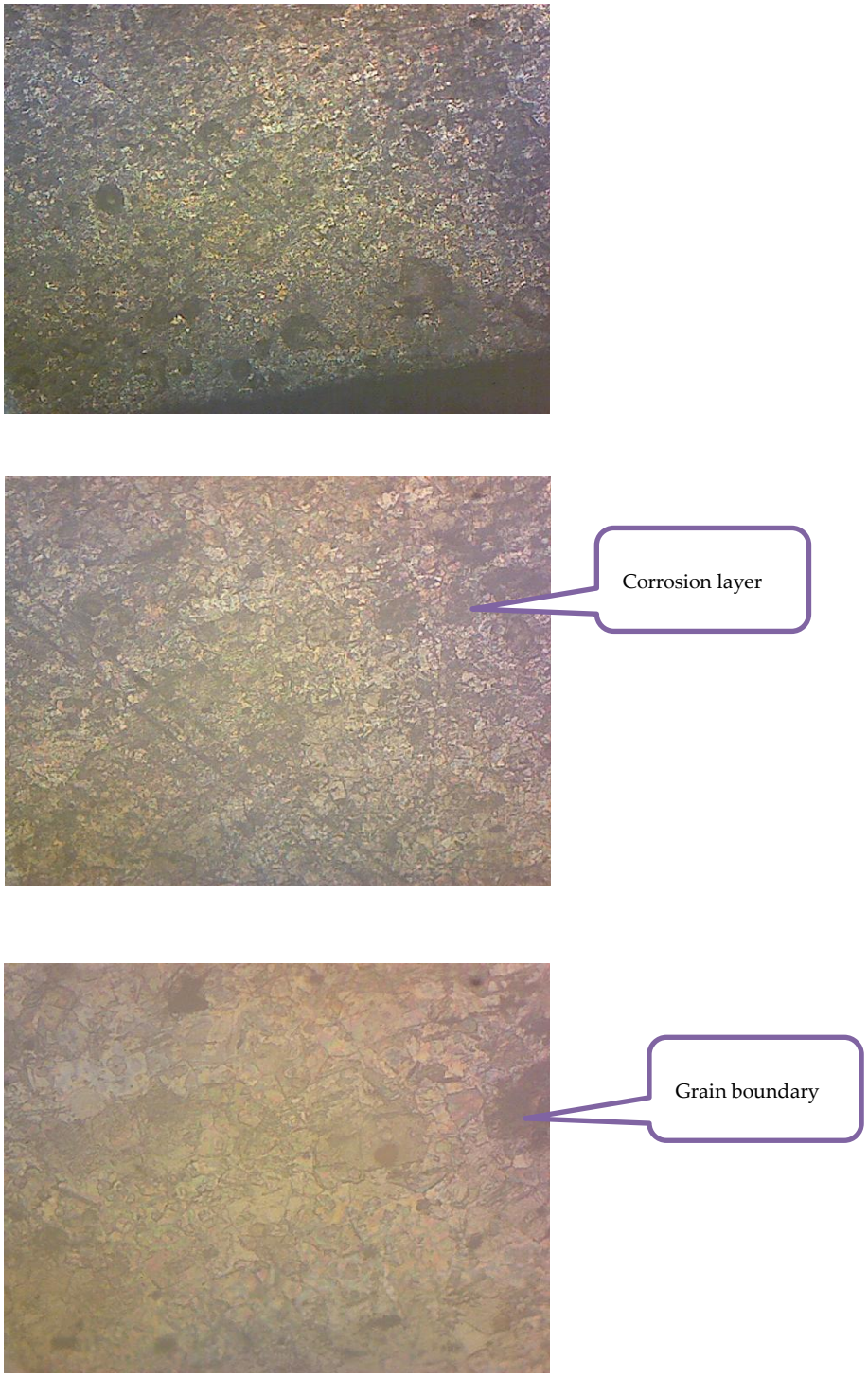

Figure 59: Observed microstructure of AR samples of 16 SWG (1.4 mm)

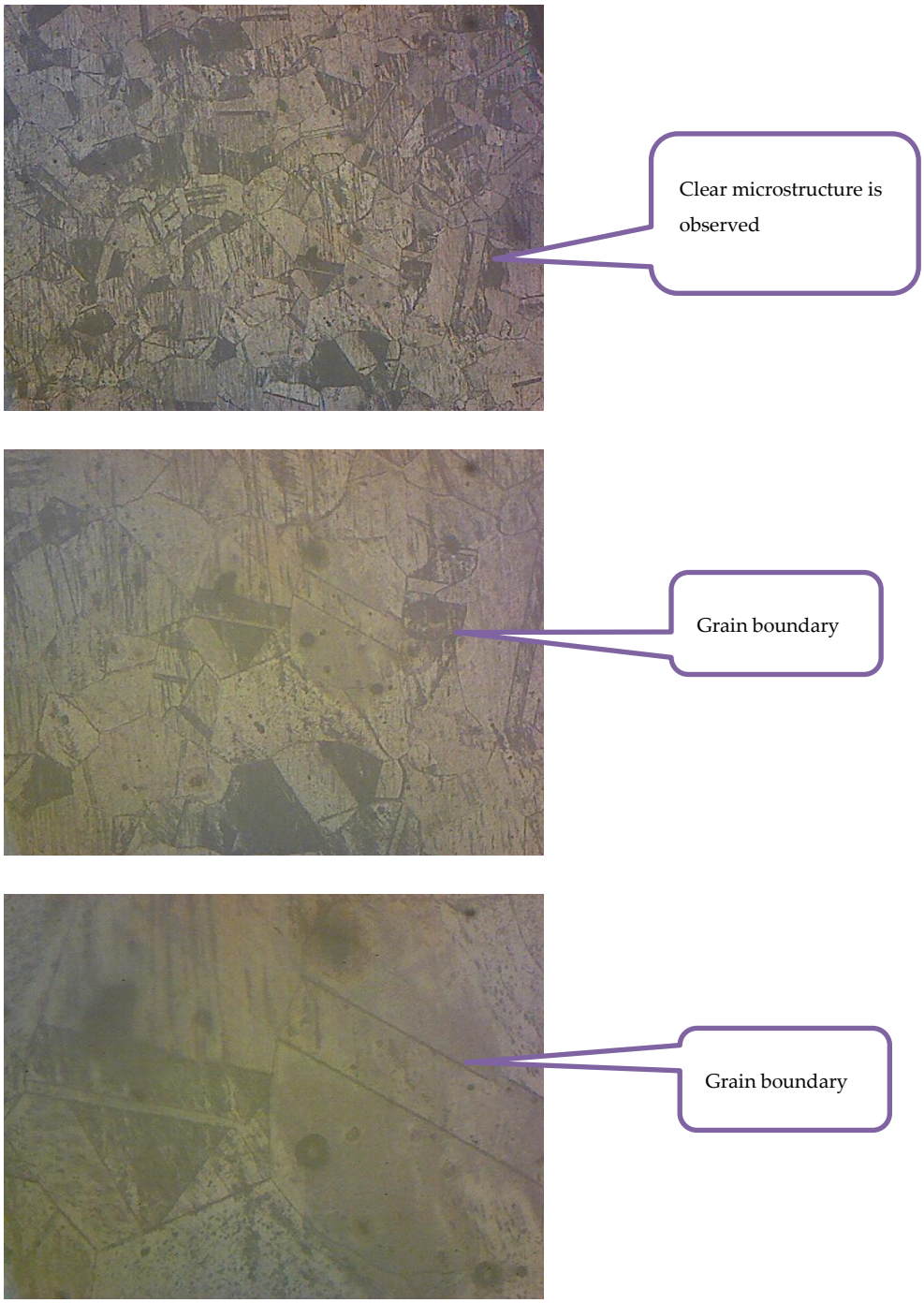

Figure 60: Observed microstructure of AP samples of 16 SWG (1.4 mm)

7.8 Forming Limit Diagram (FLD)

On the basis of measurement of major and minor axes as discussed above, Forming limit diagram of As Annealed and Pickled (AP) specimen of 0.6 mm thickness was drawn (Figure 61)

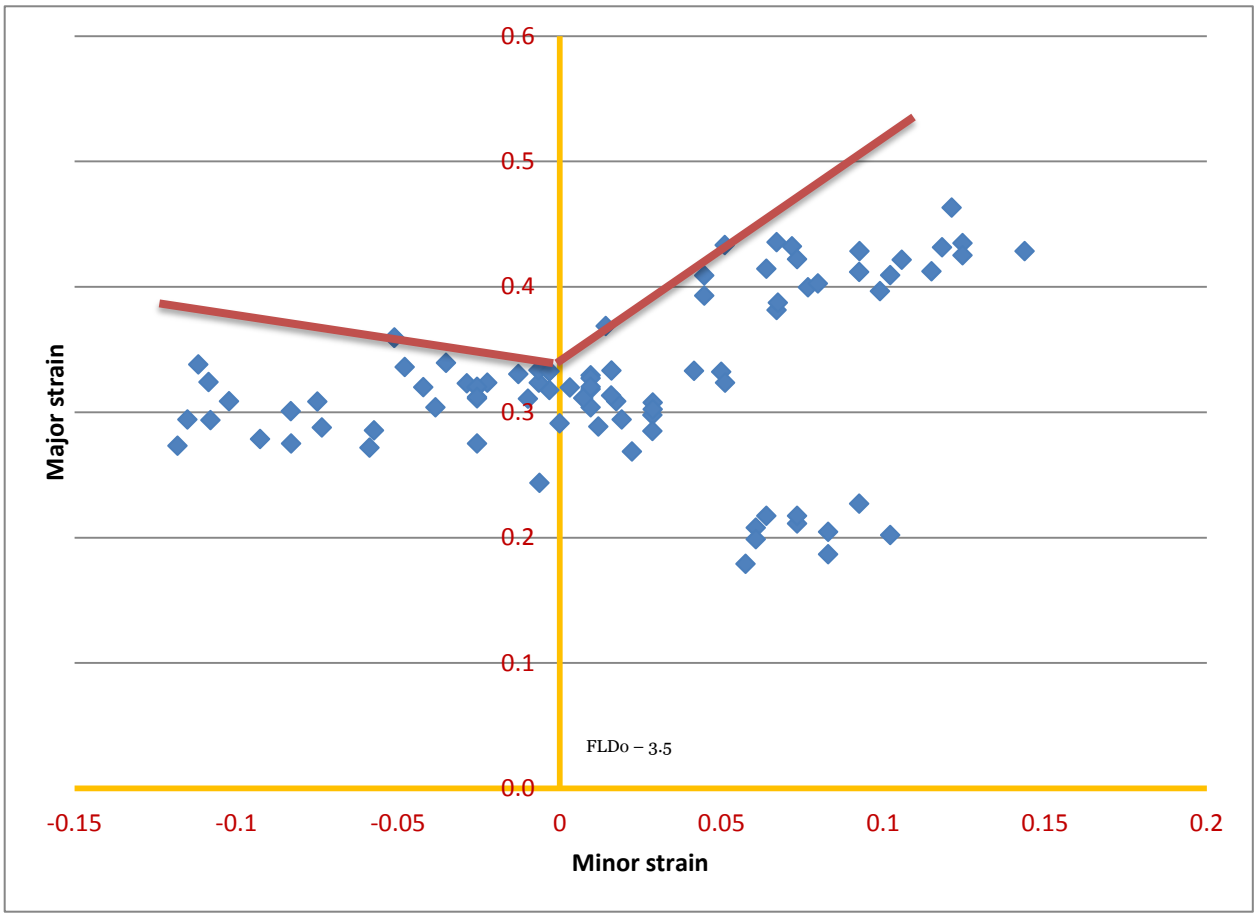

Figure 61: Forming Limit Diagram (FLD)

It can be observed that Forming Limit Curve was obtained at FLDo – 3.5 (Major strain at which minor strain is zero). It can be seen that all the strains were below the Forming Limit Curve. This result was mainly due to the fact that all the forming experiment were performed in the safe condition i.e. just before the possibility of cracking condition. The Limiting Dome Height (LDH) was experimental found out to be 24.88 mm. The dome heights of the specimens (in safe condition) used for testing are provided in Table 5.

Table 5: Dome height of the specimens

Specimen details	Dome height (Safe condition) (mm)
100mm x 100mm	24.85
100mm x 80 mm	27.27
100mm x 60 mm	23.97
100mm x 40mm	18.73
100mm x 20mm	17.63

7.9 Finite Element Analysis (FEA)

In the failure analysis in FEA, the LDH value obtained is in line with the experimentally determined LDH. The progressive safe and failure points in the simulation are shown in Figure 62.

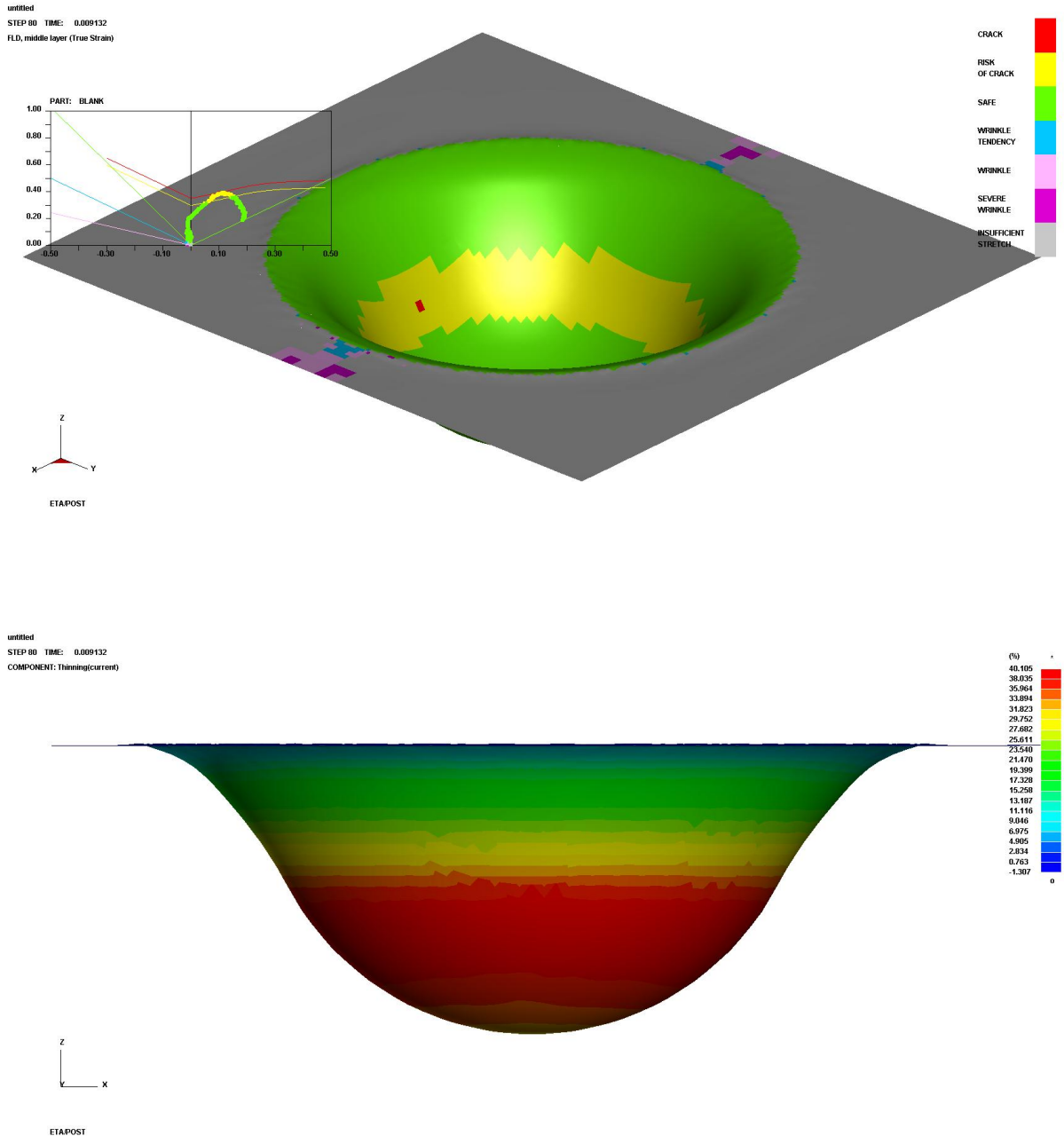

Figure 62: Picture of parameters used in FEA software

8. Conclusions

Following conclusions can be drawn from the experimental results:

- The yield strength of AISI202 As Annealed & Pickled (AP) sheet was obtained by using 0.2% offset method and is approximately 378MPa on an average basis. Individual average yield stress ranged 298.6 – 345.7 MPa for 16 SWG sheets, 379.5 – 395 MPa for 20 SWG sheets and 219 – 268.3 MPa for 22 SWG sheets. The sheets are not highly anisotropic although some variations are seen in the yield stress which may occur due to material batch inconsistency.
- Ultimate tensile strength was determined by maximum load and original cross section area of the AP specimen and is found to be in the order of 800 - 1000MPa on an average. Average UTS ranged 914 – 976.3 MPa for 16 SWG sheets, 892.6 – 954.2 MPa for 20 SWG sheets and 818 – 893 MPa for 22 SWG sheets. The ultimate tensile strength of the material is very high suggesting higher forming loads and better formability characteristics.
- Normal anisotropy of AP specimens was found to be 0.9492 for 16 SWG sheets, 0.9536 for 20 SWG sheets and 0.8464 for 22 SWG sheets. This determines thinning behaviour of sheet metals during stretching and it is an important parameter in deep-drawing operations. The material is almost isotropic which is not good for deep drawability, although multistage draw with intermediate annealing is advisable.
- Planar anisotropy of AP specimen was found to be 0.0319 for 16 SWG sheets, -0.0416 for 20 SWG sheets and 0.0491for 22 SWG sheets. Planar anisotropy has minor but important effect on drawability. Higher the value of planar anisotropy, the more earing occurs. Thus this increases the need for trimming and reduces the total depth of draw. The planar anisotropy of these sheets is comparatively low and they are suitable for deep drawing operations.
- Average yield stress of As Rolled (AR) sheets of 22 SWG specimens were in the range of 931 – 1146 MPa and average UTS were in the range of 1328 – 1411 MPa. For 20 SWG specimens average yield stress were in the range of 1374 – 1408 MPa and UTS were in the range of 1418 – 1481 MPa. For 16 SWG average yield stress were in the range of 793 – 864 MPa and average UTS were in the range of 1109 – 1171 MPa
- The planner anisotropy of AR 22 SWG specimen was found to be -0.15153 and normal anisotropy was found to be 0.930722. The planner anisotropy of 20 SWG specimen was found to be 0.802216 and normal anisotropy was found to be 0.611428. The planner anisotropy of 16 SWG specimen was found to be 0.064237 and normal anisotropy was found to be 0.57575.
- All the tensile specimens showed neck free uniform elongation of approximately 59.6% resulting in abrupt fracture at the end of the tensile test.
- Planar anisotropy increases with increase in plastic strain depicting the earing tendency in AISI202.
- Normal anisotropy increases with increase in plastic strain, although the increase is nominal but accurate.
- Highest plastic strain is observed in specimen orientation at 90° to rolling direction followed by orientations of 0° and 45° respectively.

- Average yield stresses of AR specimens are almost 3.5 times of average yield stress of AP specimens. Average ultimate yield stresses of AR specimens are almost 1.4 times of average ultimate yield stress of AP specimens.
- The microstructure of AP specimens have well defined grain boundaries.
- Well defined grain boundary was visible in 16 SWG specimens
- FLDo of the specimen was 3.5 (Major strain at which minor strain is zero).
- It can be seen that all the strains were below the Forming Limit Curve. This result was mainly due to the fact that all the forming experiment were performed in the safe condition i.e. just before the possibility of cracking condition.
- The Limiting Dome Height (LDH) was experimental found out to be 24.88 mm which was in agreement with the LDH value obtained in the simulation.

9. Scope of future study

- Forming analysis of specimens at each stage of gauge reduction
- Experiments for determining FLD for each stage of gauge reduction
- Prediction of FLD using various a theoretical method
- Grain size determination

10. References

Aleksandrovic S, Stefanovic M, Adamovic D, Lazic V. Variation of normal anisotropy ratio 'r' during plastic forming. Strojniski vestnik- journal of mechanical engineering. 2009;55(6):392-399.

ASTM-E517:2006. Standard test method for plastic strain ratio r for sheet metal.

B.L.Juneja, 2010, Fundamentals of Metal Forming Processes, New Age International Publisher, ISBN978-81-224-3089-9.

Dieter GE. Mechanical Metallurgy. 3rd ed. London: McGraw-Hill; 1988.

Ducan J.L, Other techniques for measuring n, Sheet Met. Ind., July 1967, pp 483 – 489; taken from Dieter GE. Mechanical Metallurgy. 3rd ed. London: McGraw-Hill; 2013; pp 287.

Feliksstachowicz,"Formability of aluminium alloy sheets", journal of mechanical working technology,13(1986)229-235.

Gautam, V. 2014. Tensile behaviour of austenitic stainless steel, Proceeding of International Conference on Advance Trends in Engineering & Technology (ICATET-2014), ISBN 978-81-925882-2-3.

HeckerS.S.,Met. Eng. Q. 14 (1974) 30.

Hosford WF, Caddell RM. Metal Forming Mechanics and Metallurgy. 3th ed. New York: Cambridge; 2007.

http://www.kadindia.com/ss200vsss304.html

Huh J, Huh H, Lee CS. Effect of strain rate on plastic anisotropy of advanced high strength steel sheets. International Journal of Plasticity. 2013;44:23-46.

Kalpakjian.S, Schmid.S.R., Manufacturing Engineering and Technology, 2006, 4th Edi, Pearson Edu

KEELER, S.P., UNDERSTANDING SHEET-METAL FORMABILITY, SHEET METAL INDUSTRIES, 1971, VOL. 48, NOS. 5-10

Lo KH, Shek CH, Lai JKL. Recent developments in stainless steels. Materials Science and Engineering: R. 2009;65:39-104.

Neto DM, Oliveira MC, Alves JL, Menezes LF. Influence of the plastic anisotropy modelling in the reverse deep drawing process simulation. Materials and Design. 2014;60:368–379.

Padmanabhan R, Baptista AJ, Oliveira MC, Menezes LF. Effect of anisotropy on the deep-drawing of mild steel and dual-phase steel tailor-welded blanks. Journal of Materials Processing Technology. 2007;184:288–293.

Low R, Garofalo F. Proc. Soc. Exp, Stress Anal, vol. 4, no 2, pp 16 – 25, 1947, taken from Dieter GE. Mechanical Metallurgy. 3rd ed. London: McGraw-Hill; 2013; pp 287.

Saxena RK, Dixit PM. Finite element simulation of earing defect in deep drawing. The International Journal of Advanced Manufacturing Technology. 2009;45(3-4):219-223.

Sing W.M. and Rao K.P.," Prediction of sheet metal formability by tensile test results", Journal of Materials Processing Technology, 37 (1993) 37 51.

SUDHAKARAN. R, SIVASAKTHIVEL. P.S, NAGARAJA.S and EAZHIL. K.M, The Effect of Welding Process Parameters on Pitting Corrosion and Microstructure of Chromium-Manganese Stainless Steel Gas Tungsten Arc Welded Plates, Procedia Engineering 97 (2014) 790 – 799.

World Steel Association (2015), "WORLD STEEL IN FIGURES 2015", ISBN 978-2-930069-82-1

Tisza, M., Kovacs, Z.P., 2012.New Methods for predicting the formability of sheet metals, J. Prod. Process & Sys, 5 (1) 45-54.

http://www.metalformingmagazine.com/assets/issue/images/2015/03/Science/Fig-3.jpg, assessed on 28 July 2016

http://www.metalformingmagazine.com/magazine/article.asp?aid=9277, assessed on 31 July 2016